

Slepian Spatial-Spectral Concentration on the Ball

Zubair Khalid^{a,1,*}, Rodney A. Kennedy^{a,1}, Jason D. McEwen^{b,2}

^a*Research School of Engineering, College of Engineering and Computer Science, The Australian National University, Canberra, Australia.*

^b*Mullard Space Science Laboratory, University College London, Surrey RH5 6NT, UK.*

Abstract

We formulate and solve the analogue of Slepian spatial-spectral concentration problem on the three-dimensional ball. Both the standard Fourier-Bessel and also the Fourier-Laguerre spectral domains are considered since the latter exhibits a number of practical advantages such as spectral decoupling and exact computation. The Slepian spatial and spectral concentration problems are formulated as eigenvalue problems, the eigenfunctions of which form an orthogonal family of concentrated functions. Equivalence between the spatial and spectral problems is shown. The spherical Shannon number on the ball is derived, which acts as the analog of the space-bandwidth product in the Euclidean setting, giving an estimate of the number of concentrated eigenfunctions and thus the dimension of the space of functions that can be concentrated in both the spatial and spectral domains simultaneously. Various symmetries of the spatial region are considered that reduce considerably the computational burden of recovering eigenfunctions, either by decoupling the problem into smaller subproblems or by affording analytic calculations. The family of concentrated eigenfunctions forms a Slepian basis that can be used to represent concentrated signals efficiently. We illustrate our results with numerical examples and show that the Slepian basis indeed permits a sparse representation of concentrated signals.

Keywords: Slepian concentration problem; band-limited function; eigenvalue problem; harmonic analysis; ball

1. Introduction

It is well-known that functions cannot have finite support in both the spatial (or time) and spectral (or frequency) domain at the same time [42, 41]. The fundamental problem of finding and representing the functions that are optimally energy concentrated in both the time and frequency domains was solved by Slepian, Landau and Pollak in the early 1960s [42, 18, 19, 43]. This problem, herein referred to as the *Slepian*

*Corresponding author

Email addresses: zubair.khalid@anu.edu.au (Zubair Khalid), rodney.kennedy@anu.edu.au (Rodney A. Kennedy), jason.mcewen@ucl.ac.uk (Jason D. McEwen)

¹Supported by the Australian Research Council's Discovery Projects funding scheme (project no. DP1094350).

²Supported in part by a Newton International Fellowship from the Royal Society and the British Academy.

spatial-spectral concentration problem, or *Slepian concentration problem* for short, gives rise to the orthogonal families of functions that are optimally concentrated in the spatial (spectral) domain and exactly limited in the spectral (spatial) domain. These families of functions and their multidimensional extensions [40, 39] have been used extensively in various branches of science and engineering (e.g., signal processing [46, 25], medical imaging [15], geophysics [48], climatology [47], to name a few). Notably, they have been used in linear inverse problems [13], interpolation [28, 35, 34], extrapolation [53] and in solving partial differential equations [5, 7]. Indeed, in many scientific and engineering applications, these functions have become the preferred spatial or spectral windows for the regularization of quadratic inverse problems of power spectral estimation from spatially limited observations [48, 31].

Although the Slepian spatial-spectral concentration problem was initially formulated and solved in the Euclidean domain, generalizations for various geometries and connections to wavelet analysis have also been well-studied (e.g., [27, 11, 8, 12, 3, 29, 30, 51, 36]). We note that the Slepian concentration problem for functions defined on the two-sphere \mathbb{S}^2 has been thoroughly revisited and investigated [3, 36, 51]. The resulting orthogonal family of band-limited spatially concentrated functions have been applied for localised spectral analysis [52] and spectral estimation [10] of signals (finite energy functions) defined on the sphere. There are also many applications [22, 38, 37] where signals or data are defined naturally on the three-dimensional ball, or ball for short. For example, signals defined on the ball arise when observations made on the sphere are augmented with radial information, such as depth, distance or redshift. Recently, a number of signal processing techniques have been tailored and extended to deal with signals defined on the ball (e.g., [38, 21, 22]).

In this paper, we pose, solve and analyse the Slepian concentration problem of simultaneous spatial and spectral localisation of functions defined on the ball. By considering Slepian's quadratic (energy) concentration criterion, we formulate and solve the problems to: (1) find the band-limited functions with maximum concentration in some spatial region; and (2) find the space-limited functions with maximum concentration in some region of the spectral domain. Each problem is formulated as an eigenvalue problem, the solution of which gives the orthogonal family of functions, referred to as eigenfunctions, which are either spatially concentrated while band-limited, or spectrally concentrated while space-limited. These eigenfunctions serve as an alternative basis on the ball, which we call a Slepian basis, for the representation of a band-limited or space-limited signal. We show, and also illustrate through an example, that the representation of band-limited spatially concentrated or space-limited spectrally concentrated functions is sparse in the Slepian basis, which is the essence of the Slepian spatial-spectral concentration problem. We also derive the spherical Shannon number as an equivalent of the Shannon number in the one dimensional Slepian concentration problem [43, 31], which serves as an estimate of the number of concentrated functions in the Slepian basis.

For the spectral domain characterization of functions defined on the ball we use two basis functions: (1)

spherical harmonic-Bessel functions, which arise as a solution of Helmholtz's equation in three-dimensional spherical coordinates, and are referred to as *Fourier-Bessel*³ basis functions; and (2) spherical harmonic-Laguerre functions, which are referred to as *Fourier-Laguerre* basis functions. We consider the Fourier-Laguerre functions in addition to the standard Fourier-Bessel functions as the Fourier-Laguerre functions serve as a complete basis for signals defined on the ball, enable the decoupling of the radial and angular components of the signal, and support the exact computation of forward and inverse Fourier-Laguerre transforms [22]. We show that the eigenvalue problem to find the eigenfunctions or the Slepian basis can be decomposed into subproblems when the spatial region of interest is symmetric in nature. We consider two types of symmetric regions: (1) circularly symmetric regions; and (2) circularly symmetric and radially independent regions.

As Slepian functions on the one-dimensional Euclidean domain [42, 18, 19, 43], and other geometries [40, 27, 3, 30, 36], have been widely useful in a diverse variety of applications, we hope that the proposed orthogonal family of Slepian eigenfunctions on the ball will find similar applications in fields such as cosmology, geophysics and planetary science, where data/signals are often inherently defined on the ball. For example, the band-limited spatially concentrated eigenfunctions can be used as window functions to develop multi-window spectral estimation techniques [46, 47, 10, 51] for the estimation of the signal spectrum from observations made over the limited spatial region.

We organize the remainder of the paper as follows. The mathematical preliminaries for functions on the ball are presented in Section 2. The Slepian concentration problem is posed as an eigenvalue problem in Section 3 and the resulting eigenfunctions are analysed in Section 4. The decomposition of the eigenvalue problem into subproblems for the case of special, but important, symmetric spatial regions is presented in Section 5. The representation of spatially concentrated band-limited functions in the Slepian basis is discussed and illustrated in Section 6. Concluding remarks are made in Section 7.

2. Mathematical Preliminaries

We review the mathematical background of signals defined on the ball in this section. After defining coordinate systems, measures and inner products, we then review harmonic analysis on the ball, focusing on both the Fourier-Bessel and Fourier-Laguerre settings. We conclude this section by reviewing important subspaces and operators related to the ball.

2.1. Signals on the Sphere and Ball

We define the ball by $\mathbb{B}^3 \triangleq \mathbb{R}^+ \times \mathbb{S}^2$, where \mathbb{R}^+ denotes the domain $[0, \infty)$ on the real line and $\mathbb{S}^2 \triangleq \{\mathbf{y} \in \mathbb{R}^3: \|\mathbf{y}\| = 1\}$ denotes the unit sphere. A vector $\mathbf{r} \in \mathbb{B}^3$ can be represented in spherical coordinates

³A more appropriate terminology would be spherical harmonic-Bessel basis, however we adopt the established convention of using the term Fourier to denote the spherical harmonic part.

as $\mathbf{r} \equiv \mathbf{r}(r, \theta, \phi) \triangleq (r \sin \theta \cos \phi, r \sin \theta \sin \phi, r \cos \theta)^T$, where $(\cdot)^T$ denotes matrix or vector transpose. Here, $r \triangleq \|\mathbf{r}\| \in [0, \infty)$ represents the Euclidean norm of \mathbf{r} , $\theta \in [0, \pi]$ represents the co-latitude or elevation measured with respect to the positive z -axis and $\phi \in [0, 2\pi)$ represents the longitude or azimuth and is measured with respect to the positive x -axis in the x - y plane. The unit norm vector $\hat{\mathbf{r}} \equiv \hat{\mathbf{r}}(\theta, \phi) \triangleq \mathbf{r}/\|\mathbf{r}\| = (\sin \theta \cos \phi, \sin \theta \sin \phi, \cos \theta)^T \in \mathbb{R}^3$ represents a point on the unit sphere \mathbb{S}^2 .

The space of square integrable complex-valued functions defined on \mathbb{R}^+ , \mathbb{S}^2 and \mathbb{B}^3 form Hilbert spaces, denoted by $L^2(\mathbb{R}^+)$, $L^2(\mathbb{S}^2)$ and $L^2(\mathbb{B}^3)$, respectively, equipped with the inner products defined by

$$\langle f, g \rangle_{\mathbb{R}^+} \triangleq \int_{\mathbb{R}^+} dv(r) f(r) g^*(r), \quad (1)$$

$$\langle f, g \rangle_{\mathbb{S}^2} \triangleq \int_{\mathbb{S}^2} d^2\nu(\hat{\mathbf{r}}) f(\hat{\mathbf{r}}) g^*(\hat{\mathbf{r}}), \quad (2)$$

$$\langle f, g \rangle_{\mathbb{B}^3} \triangleq \int_{\mathbb{B}^3} d^3\mu(\mathbf{r}) f(\mathbf{r}) g^*(\mathbf{r}), \quad (3)$$

where f, g are functions respectively defined on \mathbb{R}^+ , \mathbb{S}^2 and \mathbb{B}^3 in (1), (2) and (3), $dv(r) = r^2 dr$, $d^2\nu(\hat{\mathbf{r}}) = \sin \theta d\theta d\phi$ and $d^3\mu(\mathbf{r}) = r^2 \sin \theta dr d\theta d\phi$ represents infinitesimal length, area and the volume element respectively, $(\cdot)^*$ denotes complex conjugation and the integration is carried out over the respective domain. The inner products in (1), (2) and (3) induce norms $\|f\| \triangleq \langle f, f \rangle^{1/2}$. Throughout this paper, the functions with finite induced norm belonging to one of these spaces are referred to as signals.

2.2. Harmonic Analysis on the Ball

We review harmonic analysis on the ball, starting with the spherical Bessel and Laguerre transforms on the positive real line \mathbb{R}^+ and the spherical harmonic transform on the unit sphere \mathbb{S}^2 , before combining these to recover the Fourier-Bessel and Fourier-Laguerre transforms on the ball, respectively.

2.2.1. Spherical Bessel Transform

The spherical Bessel functions, which arise as radial solutions to the Helmholtz equation in spherical coordinates, form a basis for functions on the non-negative real line \mathbb{R}^+ . In this work, we consider spherical Bessel functions of the first kind, denoted by j_ℓ defined on \mathbb{R}^+ , where ℓ denotes the order. The spherical Bessel functions satisfy the closure relation [49]

$$\int_{\mathbb{R}^+} dv(r) j_\ell(kr) j_\ell(k'r) = \frac{\pi}{2k^2} \delta(k - k'), \quad (4)$$

for $r \in \mathbb{R}^+$ and $k \in \mathbb{R}^+$, and where $\delta(k - k')$ denotes the one-dimensional Dirac delta. Consequently, we can represent a signal $f \in L^2(\mathbb{R}^+)$ using the following ℓ -th order spherical Bessel inverse and forward transform, respectively,

$$f(r) = \sqrt{\frac{2}{\pi}} \int_{\mathbb{R}^+} dk f_\ell(k) k j_\ell(kr) \quad \text{with} \quad f_\ell(k) \triangleq \sqrt{\frac{2}{\pi}} \int_{\mathbb{R}^+} dv(r) f(r) k j_\ell(kr), \quad (5)$$

where $f_\ell(k)$ denotes the spherical Bessel transform.

2.2.2. Spherical Laguerre Transform

The Laguerre polynomials, solutions to the Laguerre differential equation [32, 50], are well known for their various applications, notably in the quantum mechanical treatment of the hydrogen atom [14], and form a basis for functions on the interval \mathbb{R}^+ . We adopt the spherical Laguerre transform and associated normalisation presented by [22], defining the spherical Laguerre basis functions of non-negative integer radial degree p by

$$K_p(r) \triangleq \sqrt{\frac{p!}{(p+2)!}} e^{-r/2} L_p^{(2)}(r), \quad (6)$$

where $L_p^{(2)}(r)$ represents the p -th generalized Laguerre polynomial of second order, defined by

$$L_p^{(2)}(r) \triangleq \sum_{j=0}^p \binom{p+2}{p-j} \frac{(-r)^j}{j!}. \quad (7)$$

Since we use the spherical Laguerre basis functions for the expansion of signals defined on \mathbb{R}^+ with differential measure $dv(r) = r^2 dr$, we have chosen the second order generalized Laguerre polynomial. The basis functions $K_p(r)$ in (6) are orthonormal on \mathbb{R}^+ , that is, $\langle K_p, K_q \rangle_{\mathbb{R}^+} = \delta_{pq}$, where δ_{pq} denotes the Kronecker delta. The spherical Laguerre polynomials defined in (6) serve as complete basis functions on \mathbb{R}^+ , where the completeness stems from the completeness of generalized Laguerre polynomials and therefore we can expand a signal $f \in L^2(\mathbb{R}^+)$ using the following spherical Laguerre inverse and forward transform, respectively,

$$f(r) = \sum_{p=0}^{\infty} f_p K_p(r) \quad \text{with} \quad f_p \triangleq \langle f, K_p \rangle_{\mathbb{R}^+}, \quad (8)$$

where f_p denotes the spherical Laguerre coefficient of radial degree p .

2.2.3. Spherical Harmonic Transform

The spherical harmonic functions, which arise as angular solutions to the Helmholtz's equation in spherical coordinates, are denoted $Y_\ell^m(\hat{\mathbf{x}}) = Y_\ell^m(\theta, \phi)$, for integer degree $\ell \geq 0$ and integer order $|m| \leq \ell$ and are defined by [9, 33, 16]

$$Y_{\ell m}(\hat{\mathbf{r}}) = Y_{\ell m}(\theta, \phi) = \sqrt{\frac{2\ell+1}{4\pi} \frac{(\ell-m)!}{(\ell+m)!}} P_\ell^m(\cos \theta) e^{im\phi}, \quad (9)$$

where P_ℓ^m denotes the associated Legendre function of degree ℓ and order m with Condon-Shortley phase included [16]. With the above definition, the spherical harmonic functions, or simply the spherical harmonics, form a complete orthonormal basis for $L^2(\mathbb{S}^2)$ and therefore a signal $f \in L^2(\mathbb{S}^2)$ can be expanded using the following spherical harmonic inverse and forward transform, respectively,

$$f(\hat{\mathbf{r}}) = \sum_{\ell=0}^{\infty} \sum_{m=-\ell}^{\ell} f_{\ell m} Y_{\ell m}(\hat{\mathbf{r}}) \quad \text{with} \quad f_{\ell m} \triangleq \langle f, Y_{\ell m} \rangle_{\mathbb{S}^2}, \quad (10)$$

where $f_{\ell m}$ denotes the spherical harmonic coefficient of angular degree ℓ and order m . We note that the spherical harmonic functions follow the conjugate symmetry property $Y_{\ell m}(\hat{\mathbf{r}}) = (-1)^m Y_{\ell(-m)}^*(\hat{\mathbf{r}})$. We further note that the function f is real valued if its spherical harmonic coefficients satisfy the conjugate symmetry property $f_{\ell m} = (-1)^m f_{\ell(-m)}^*$.

2.2.4. Fourier-Bessel Transform

We define the Fourier-Bessel functions, which arise as a solution of Helmholtz's equation in three-dimensional spherical coordinates, as [6, 23, 1]

$$X_{\ell m}(k, \mathbf{r}) \triangleq \sqrt{\frac{2}{\pi}} k j_{\ell}(kr) Y_{\ell m}(\theta, \phi), \quad \mathbf{r} = \mathbf{r}(r, \theta, \phi). \quad (11)$$

With the above definition, the Fourier-Bessel functions form a complete, orthogonal basis for $L^2(\mathbb{B}^3)$, satisfying the orthogonality relation

$$\int_{\mathbb{B}^3} d^3\mu(\mathbf{r}) X_{\ell m}(k, \mathbf{r}) X_{\ell' m'}^*(k', \mathbf{r}) = \delta(k - k') \delta_{\ell\ell'} \delta_{mm'}. \quad (12)$$

By the completeness of the Fourier-Bessel functions, a signal $f \in L^2(\mathbb{B}^3)$ can be decomposed in the Fourier-Bessel basis by

$$\begin{aligned} f(\mathbf{r}) &= \int_{\mathbb{R}^+} dk \sum_{\ell=0}^{\infty} \sum_{m=-\ell}^{\ell} f_{\ell m}(k) X_{\ell m}(k, \mathbf{r}) \\ &= \sqrt{\frac{2}{\pi}} \int_{\mathbb{R}^+} dk \sum_{\ell=0}^{\infty} \sum_{m=-\ell}^{\ell} f_{\ell m}(k) k j_{\ell}(kr) Y_{\ell m}(\theta, \phi) \end{aligned} \quad (13)$$

where $f_{\ell m}(k)$ denotes the Fourier-Bessel coefficient, of degree ℓ , order m and radial harmonic variable $k \in \mathbb{R}^+$, given by

$$f_{\ell m}(k) \triangleq \sqrt{\frac{2}{\pi}} \int_{\mathbb{B}^3} d^3\mu(\mathbf{r}) f(\mathbf{r}) k j_{\ell}(kr) Y_{\ell m}^*(\theta, \phi). \quad (14)$$

The Fourier-Bessel coefficients constitute a spectral domain representation of signals defined on the ball. Such a spectral domain is referred as the *Fourier-Bessel spectral domain*.

The Fourier-Bessel transform is the natural (standard) harmonic transform on the ball since the Fourier-Bessel functions are the eigenfunctions of the spherical Laplacian and thus the Fourier-Bessel transform corresponds to the standard three-dimensional Fourier transform in spherical coordinates. However, the Fourier-Bessel transform suffers from a number of practical limitations [22], motivating alternative harmonic representations of the ball, such as the Fourier-Laguerre transform.

2.2.5. Fourier-Laguerre Transform

In the Fourier-Bessel transform, the spherical Bessel functions are used for the decomposition of a signal along the radial line \mathbb{R}^+ . Alternatively, we can use the spherical Laguerre basis functions for the expansion

of a signal along \mathbb{R}^+ . Combining the spherical Laguerre basis functions and spherical harmonic functions, we define the Fourier-Laguerre basis functions for a signal as

$$Z_{\ell mp}(\mathbf{r}) \triangleq K_p(r)Y_\ell^m(\theta, \phi), \quad \mathbf{r} = \mathbf{r}(r, \theta, \phi). \quad (15)$$

By the completeness of both Laguerre polynomials and spherical harmonics, any signal $f \in L^2(\mathbb{B}^3)$ can be expanded as [22]

$$f(\mathbf{r}) = \sum_{p=0}^{\infty} \sum_{\ell=0}^{\infty} \sum_{m=-\ell}^{\ell} f_{\ell mp} Z_{\ell mp}(\mathbf{r}), \quad (16)$$

where $f_{\ell mp}$ is the Fourier-Laguerre coefficient of radial degree p , angular degree ℓ and angular order m , and is obtained by the Fourier-Laguerre transform

$$f_{\ell mp} \triangleq \langle f, Z_{\ell mp} \rangle_{\mathbb{B}^3} = \int_{\mathbb{B}^3} d^3\mu(\mathbf{r}) f(\mathbf{r}) Z_{\ell mp}^*(\mathbf{r}). \quad (17)$$

These Fourier coefficients constitute another spectral domain representation of signals defined on the ball, which we refer to as the *Fourier-Laguerre spectral domain*.

The Fourier-Laguerre transform exhibits a number of practical advantages over the Fourier-Bessel transform, namely: (1) the angular and radial components of signals are decoupled in harmonic space; and (2) exact quadrature can be developed, leading to theoretically exact forward and inverse Fourier-Laguerre transforms [22].

2.2.6. Dirac Delta on the Ball

The Dirac delta function on the ball is defined by

$$\delta(\mathbf{r}, \mathbf{r}') \triangleq (r^2 \sin \theta)^{-1} \delta(r - r') \delta(\theta - \theta') \delta(\phi - \phi'), \quad (18)$$

and satisfies the sifting property

$$\int_{\mathbb{B}^3} d^3\mu(\mathbf{r}') f(\mathbf{r}') \delta(\mathbf{r}, \mathbf{r}') = f(\mathbf{r}). \quad (19)$$

The Dirac delta has the following expansion in terms of Fourier-Bessel basis functions

$$\begin{aligned} \delta(\mathbf{r}, \mathbf{r}') &= \sum_{\ell=0}^{\infty} \sum_{m=-\ell}^{\ell} \int_{\mathbb{R}^+} dk X_{\ell m}(k, \mathbf{r}) X_{\ell m}^*(k, \mathbf{r}') \\ &= \frac{1}{2\pi^2} \sum_{\ell=0}^{\infty} (2\ell + 1) P_\ell^0(\hat{\mathbf{r}} \cdot \hat{\mathbf{r}}') \left(\int_{\mathbb{R}^+} dk k^2 j_\ell(kr) j_\ell(kr') \right), \end{aligned} \quad (20)$$

and has the following expansion in terms of Fourier-Laguerre basis functions

$$\begin{aligned} \delta(\mathbf{r}, \mathbf{r}') &= \sum_{p=0}^{\infty} \sum_{\ell=0}^{\infty} \sum_{m=-\ell}^{\ell} Z_{\ell mp}(\mathbf{r}) Z_{\ell mp}^*(\mathbf{r}') \\ &= \sum_{p=0}^{\infty} K_p(r) K_p(r') \sum_{\ell=0}^{\infty} \frac{2\ell + 1}{4\pi} P_\ell^0(\hat{\mathbf{r}} \cdot \hat{\mathbf{r}}'), \end{aligned} \quad (21)$$

where $\hat{\mathbf{r}} \cdot \hat{\mathbf{r}}'$ denotes the three dimensional dot product between unit vectors $\hat{\mathbf{r}}$ and $\hat{\mathbf{r}}'$ and we have noted the addition theorem for the spherical harmonics.

2.3. Important Subspaces of $L^2(\mathbb{B}^3)$

Define $\tilde{\mathcal{H}}_{KL}$ as the space of band-limited functions such that the signal is band-limited in the Fourier-Bessel spectral domain within the spectral region $\tilde{A}_{KL} \triangleq \{0 \leq k \leq K, 0 \leq \ell \leq L-1\}$ for $L \in \mathbb{Z}^+$ and $K \in \mathbb{R}^+$. Due to the continuous Fourier-Bessel spectral domain k , $\tilde{\mathcal{H}}_{KL}$ is an infinite dimensional subspace of $L^2(\mathbb{B}^3)$. Define \mathcal{H}_{PL} as the space of band-limited functions such that the signal is band-limited in the Fourier-Laguerre spectral domain within the spectral region $A_{PL} \triangleq \{0 \leq p \leq P-1, 0 \leq \ell \leq L-1\}$ for $P, L \in \mathbb{Z}^+$. \mathcal{H}_{PL} is a finite dimensional subspace of $L^2(\mathbb{B}^3)$ with size PL^2 . Also define \mathcal{H}_R as the space of finite energy space-limited functions confined within the region $R \subset \mathbb{B}^3$. \mathcal{H}_R is an infinite dimensional subspace of $L^2(\mathbb{B}^3)$.

2.4. Important Operators of $L^2(\mathbb{B}^3)$

Define an operator S for signals on the ball by the general Fredholm integral equation [16]

$$(Sf)(\mathbf{r}) = \int_{\mathbb{B}^3} d^3\mu(\mathbf{r}') S(\mathbf{r}, \mathbf{r}') f(\mathbf{r}'), \quad (22)$$

where $S(\mathbf{r}, \mathbf{r}')$ is the kernel for an operator S defined on $\mathbb{B}^3 \times \mathbb{B}^3$.

Definition 1 (Spatial Selection Operator). *Define the spatial selection operator S_R , which selects the function in a volume region $R \subset \mathbb{B}^3$, with kernel $S_R(\mathbf{r}, \mathbf{r}')$ as*

$$S_R(\mathbf{r}, \mathbf{r}') \triangleq I_R(\mathbf{r})\delta(\mathbf{r}, \mathbf{r}'), \quad (23)$$

where $I_R(\mathbf{r}) = 1$ for $\mathbf{r} \in R$ and $I_R(\mathbf{r}) = 0$ for $\mathbf{r} \in \mathbb{B}^3 \setminus R$ is an indicator function of the region R . S_R projects the signal $f \in L^2(\mathbb{B}^3)$ onto the subspace \mathcal{H}_R .

Definition 2 (Fourier-Bessel Spectral Selection Operator). *Define the spectral selection operator \tilde{S}_{KL} , which selects the harmonic contribution of functions in the Fourier-Bessel spectral domain \tilde{A}_{KL} , by its kernel*

$$\tilde{S}_{KL}(\mathbf{r}, \mathbf{r}') \triangleq \sum_{\ell=0}^{L-1} \sum_{m=-\ell}^{\ell} \int_{k=0}^K dk X_{\ell m}(k, \mathbf{r}) X_{\ell m}^*(k, \mathbf{r}'). \quad (24)$$

The operator \tilde{S}_{KL} projects a signal onto the subspace of Fourier-Bessel band-limited functions $\tilde{\mathcal{H}}_{KL}$.

Definition 3 (Fourier-Laguerre Spectral Selection Operator). *Define the spectral selection operator S_{PL} , which selects the harmonic contribution of functions in the Fourier-Laguerre spectral domain A_{PL} , by its kernel*

$$S_{PL}(\mathbf{r}, \mathbf{r}') \triangleq \sum_{p=0}^{P-1} \sum_{\ell=0}^{L-1} \sum_{m=-\ell}^{\ell} Z_{\ell m p}(\mathbf{r}) Z_{\ell m p}^*(\mathbf{r}'). \quad (25)$$

The operator S_{PL} projects a signal onto the subspace of Fourier-Laguerre band-limited functions \mathcal{H}_{PL} .

Since both the spatial and spectral selection operators are orthogonal projection operators, they are idempotent and self-adjoint in nature. By noting the expansions of the Dirac delta in (20) and (21), it is evident that the kernels of the spectral selection operators in (24) and (25) are Dirac delta functions that are band-limited in the appropriate basis.

3. Simultaneous Concentration in Spatial and Spectral Domain

By virtue of the uncertainty principle, no function can be space-limited and band-limited simultaneously. In other words, a signal $f \in L^2(\mathbb{B}^3)$ cannot belong to the subspace \mathcal{H}_R and the subspaces \mathcal{H}_{PL} or $\tilde{\mathcal{H}}_{KL}$ at the same time. In this section we first develop a framework to determine band-limited functions $f \in \mathcal{H}_{PL}$ or $f \in \tilde{\mathcal{H}}_{KL}$ that are optimally concentrated in some spatial region $R \subset \mathbb{B}^3$. We then formulate the problem to determine space-limited functions $g \in \mathcal{H}_R$ that are optimally concentrated within the spectral region \tilde{A}_{KL} or A_{PL} . Later, we show the equivalence between these two problems and provide the harmonic domain formulations of the problems.

3.1. Spatial Concentration of Band-Limited Functions

Let $f \in L^2(\mathbb{B}^3)$ be a band-limited signal, that is, $f \in \mathcal{H}_L^K$ or $f \in \mathcal{H}_{PL}$. The energy concentration of the function f within the spatial region $R \subset \mathbb{B}^3$ is given by

$$\lambda = \frac{\langle \mathbf{S}_R f, \mathbf{S}_R f \rangle}{\langle f, f \rangle}, \quad (26)$$

which, by noting that the signal f is band-limited, can also be equivalently expressed as

$$\lambda = \frac{\langle \mathbf{S}_R \tilde{\mathbf{S}}_{KL} f, \mathbf{S}_R \tilde{\mathbf{S}}_{KL} f \rangle}{\langle \tilde{\mathbf{S}}_{KL} f, \tilde{\mathbf{S}}_{KL} f \rangle}, \quad f \in \mathcal{H}_L^K \quad (27)$$

$$\lambda = \frac{\langle \mathbf{S}_R \mathbf{S}_{PL} f, \mathbf{S}_R \mathbf{S}_{PL} f \rangle}{\langle \mathbf{S}_{PL} f, \mathbf{S}_{PL} f \rangle}, \quad f \in \mathcal{H}_{PL}, \quad (28)$$

where we have used the fact that both the spectral selection operators, $\tilde{\mathbf{S}}_{KL}$ and \mathbf{S}_{PL} are idempotent operators. It is well-known that the band-limited function f that renders the Rayleigh quotient (26) stationary is a solution of following Fredholm integral equations (eigenvalue problems), given by

$$\tilde{\mathbf{S}}_{KL} \mathbf{S}_R \tilde{\mathbf{S}}_{KL} f = \lambda f, \quad f \in \mathcal{H}_L^K, \quad (29)$$

$$\mathbf{S}_{PL} \mathbf{S}_R \mathbf{S}_{PL} f = \lambda f, \quad f \in \mathcal{H}_{PL}. \quad (30)$$

The solution of each of the eigenvalue problems in (29) and (30) yields band-limited eigenfunctions. Since the composite operator $\tilde{\mathbf{S}}_{KL} \mathbf{S}_R \tilde{\mathbf{S}}_{KL}$ (or $\mathbf{S}_{PL} \mathbf{S}_R \mathbf{S}_{PL}$) is a self-adjoint projection operator, these eigenvalues are positive and bounded above by unity. The eigenvalue associated with each eigenfunction serves as a measure of energy concentration of the eigenfunction in the spatial region R . We discuss the properties of the eigenfunctions in Section 4.

3.2. Spectral Concentration of Space-Limited Functions

Here we consider the dual of the problem posed in the previous subsection. Instead of seeking band-limited spatially concentrated functions, we seek space-limited functions with optimal concentration in some spectral region. Let $g \in \mathcal{H}_R$ be the space-limited function within the spatial region R . We maximize the concentration of g in the spectral region \tilde{A}_{KL} or A_{PL} , depending on the basis functions chosen for the characterization of the spectral domain (Fourier-Bessel or Fourier-Laguerre, respectively). To maximize the concentration of the space-limited signal g within the spectral region \tilde{A}_{KL} in the Fourier-Bessel spectral domain, we maximize the ratio

$$\lambda = \frac{\langle \tilde{S}_{KL} S_R g, \tilde{S}_{KL} S_R g \rangle}{\langle S_R g, S_R g \rangle}, \quad g \in \mathcal{H}_R. \quad (31)$$

Similarly, to maximize the concentration within the spectral region A_{PL} in the Fourier-Laguerre spectral domain, we maximize the ratio

$$\lambda = \frac{\langle S_{PL} S_R g, S_{PL} S_R g \rangle}{\langle S_R g, S_R g \rangle}, \quad g \in \mathcal{H}_R. \quad (32)$$

Following a similar approach to the spatial concentration problem above and noting $S_R g = g$, the Fourier-Bessel concentration problem in (31) results in the following eigenvalue problem

$$S_R \tilde{S}_{KL} S_R g = \lambda g. \quad (33)$$

Similarly, the Fourier-Laguerre problem in (32) gives rise to the following eigenvalue problem

$$S_R S_{PL} S_R g = \lambda g. \quad (34)$$

The solution of each of the eigenvalue problems presented in (33) and (34) provides space-limited eigenfunctions. Again, the eigenvalues are positive and bounded above by unity since the both $S_R S_{PL} S_R$ and $S_R \tilde{S}_{KL} S_R$ are self-adjoint projection operators. The eigenvalue associated with each eigenfunction serves as a measure of concentration of the eigenfunction in the spectral region A_{PL} or \tilde{A}_{KL} , as we show later in Section 4.

3.3. Equivalence of Problems

Here we show that the concentration problems to find the spatially concentrated band-limited functions and spectrally concentrated space-limited functions have equivalent solutions. Equivalence is shown explicitly only for the Fourier-Bessel spectral domain; however, the same result also holds for the Fourier-Laguerre spectral domain.

By defining a composite operator $U \triangleq \tilde{S}_{KL} S_R \tilde{S}_{KL}$ with kernel representation given by

$$\begin{aligned} U(\mathbf{r}, \mathbf{r}') &= \int_R d^3\mu(\mathbf{r}'') \tilde{S}_{KL}(\mathbf{r}, \mathbf{r}'') \tilde{S}_{KL}(\mathbf{r}'', \mathbf{r}') \\ &= \sum_{\ell=0}^{L-1} \sum_{m=-\ell}^{\ell} \sum_{\ell'=0}^{L-1} \sum_{m'=-\ell'}^{\ell'} \int_{k=0}^K dk \int_{k'=0}^K dk' X_{\ell m}(k, \mathbf{r}) X_{\ell' m'}^*(k', \mathbf{r}') \int_R d^3\mu(\mathbf{r}'') X_{\ell m}^*(k, \mathbf{r}'') X_{\ell' m'}(k', \mathbf{r}''), \end{aligned} \quad (35)$$

we can write the eigenvalue problem in (29) as

$$Uf = \lambda f, \quad (36)$$

or equivalently

$$\int_R d^3\mu(\mathbf{r}') \int_{k=0}^K dk \sum_{\ell=0}^{L-1} \sum_{m=-\ell}^{\ell} X_{\ell m}(k, \mathbf{r}) X_{\ell m}^*(k, \mathbf{r}') f(\mathbf{r}') = \lambda f(\mathbf{r}), \quad \mathbf{r} \in \mathbb{B}^3. \quad (37)$$

Also, we define the composite operator $V \triangleq S_R \tilde{S}_{KL} S_R$ with kernel representation given by

$$\begin{aligned} V(\mathbf{r}, \mathbf{r}') &= I_R(\mathbf{r}) I_R(\mathbf{r}') \sum_{\ell=0}^{L-1} \sum_{m=-\ell}^{\ell} \int_{k=0}^K dk X_{\ell m}(k, \mathbf{r}) X_{\ell m}^*(k, \mathbf{r}') \\ &= I_R(\mathbf{r}) \tilde{S}_{KL}(\mathbf{r}, \mathbf{r}'), \end{aligned} \quad (38)$$

using which the eigenvalue problem in (33) can be expressed as

$$Vg = \lambda g. \quad (39)$$

or equivalently

$$\int_R d^3\mu(\mathbf{r}') \int_{k=0}^K dk \sum_{\ell=0}^{L-1} \sum_{m=-\ell}^{\ell} X_{\ell m}(k, \mathbf{r}) X_{\ell m}^*(k, \mathbf{r}') g(\mathbf{r}') = \lambda g(\mathbf{r}), \quad \mathbf{r} \in R. \quad (40)$$

It is evident that this eigenvalue problem formulated for space-limited (analytic) function $g \in \mathcal{H}_R$ is equivalent to the problem in (37) for band-limited function $f \in \mathcal{H}_L^K$ over the domain $\mathbf{r} \in R$. Consequently, the eigenvalue problems in (36) and (39) have the same solution, with the same eigenvalue, within the region R , that is,

$$g(\mathbf{r}) = (S_R f)(\mathbf{r}), \quad \mathbf{r} \in R \subset \mathbb{B}^3. \quad (41)$$

For a signal band-limited in the Fourier-Laguerre spectral domain, the equivalent of the eigenvalue problem in (36) is

$$Wf = \lambda f, \quad (42)$$

where $W \triangleq S_{PL} S_R S_{PL}$ is the composite operator with kernel representation given by

$$\begin{aligned}
W(\mathbf{r}, \mathbf{r}') &= \int_R d^3\mu(\mathbf{r}'') S_{PL}(\mathbf{r}, \mathbf{r}'') S_{PL}(\mathbf{r}'', \mathbf{r}') \\
&= \sum_{p=0}^{P-1} \sum_{\ell=0}^{L-1} \sum_{m=-\ell}^{\ell} \sum_{p'=0}^{P-1} \sum_{\ell'=0}^{L-1} \sum_{m'=-\ell'}^{\ell'} Z_{\ell mp}(\mathbf{r}) Z_{\ell' m' p'}^*(\mathbf{r}') \int_R d^3\mu(\mathbf{r}'') Z_{\ell mp}^*(\mathbf{r}'') Z_{\ell' m' p'}(\mathbf{r}''), \quad (43)
\end{aligned}$$

and the analogous result holds.

Remark 1. *The equivalence of the spatial and spectral concentration problems implies that we only need to solve the eigenvalue problem presented in (36) or (42) to obtain the band-limited spatially concentrated eigenfunctions and the space-limited spectrally concentrated eigenfunctions then can be obtained using (41), i.e., by setting the space-limited eigenfunctions to the band-limited eigenfunctions in the region R and zero elsewhere.*

3.4. Harmonic Domain Analysis

So far the eigenvalue problems have been formulated in the spatial domain. Here we present the spectral domain formulation of the eigenvalue problems presented in (36) and (42). By taking the Fourier-Bessel transform of (37) with respect to spatial variable \mathbf{r} , we obtain the following formulation of the eigenvalue problem in the Fourier-Bessel spectral domain

$$\sum_{\ell'=0}^{L-1} \sum_{m'=-\ell'}^{\ell'} \int_{k'=0}^K dk' X_{\ell' m', \ell m}(k', k) f_{\ell' m'}(k') = \lambda f_{\ell m}(k), \quad (44)$$

with

$$X_{\ell m, \ell' m'}(k, k') = \int_R d^3\mu(\mathbf{r}) X_{\ell m}(k, \mathbf{r}) X_{\ell' m'}^*(k', \mathbf{r}). \quad (45)$$

Similarly, the eigenvalue problem (42) can be formulated in the Fourier-Laguerre spectral domain as

$$\sum_{p'=0}^P \sum_{\ell'=0}^{L-1} \sum_{m'=-\ell'}^{\ell'} Z_{\ell' m' p', \ell mp} f_{\ell' m' p'} = \lambda f_{\ell mp}, \quad (46)$$

with

$$Z_{\ell mp, \ell' m' p'} = \int_R d^3\mu(\mathbf{r}) Z_{\ell mp}(\mathbf{r}) Z_{\ell' m' p'}^*(\mathbf{r}). \quad (47)$$

By defining the vector $\mathbf{f} = (f_{000}, f_{001}, \dots, f_{(L-1)(L-1)(P-1)})^T$ of length PL^2 as the spectral representation of the signal f and the matrix \mathbf{Z} of size $PL^2 \times PL^2$ with entries given by (47), (46) can be written compactly in matrix form as

$$\mathbf{Z}\mathbf{f} = \lambda\mathbf{f}. \quad (48)$$

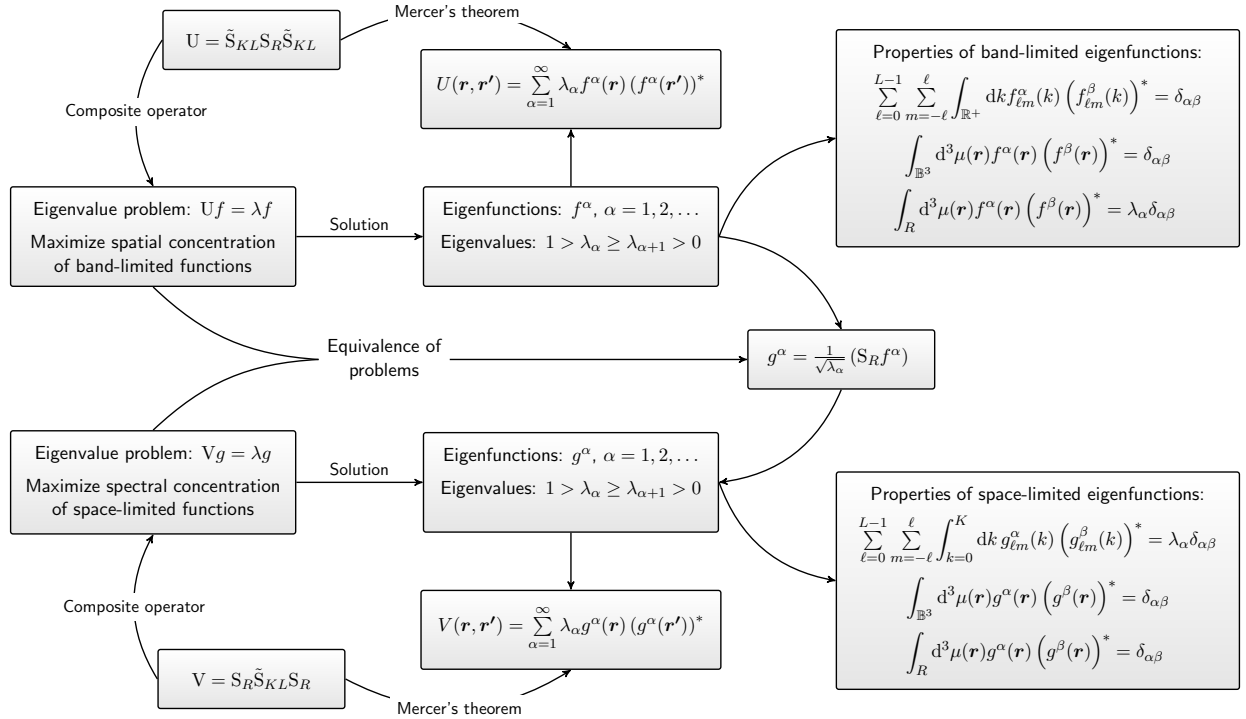


Figure 1: **Concept map of Slepian spatial-spectral concentration problem for Fourier-Bessel spectral domain** summarising the Slepian concentration problems, presented in Section 3, to find spatially concentrated band-limited functions and spectrally concentrated space-limited functions. The relation between the band-limited and space-limited eigenfunctions arising as a solution of each problem is also presented. Furthermore, the key properties of the eigenfunctions, presented in Section 4 are summarised. Employing Mercer's theorem [16], we have also shown the (convergent) representation of the kernel of the operator U or V in terms of eigenfunctions of the respective operator. The equivalent concept map can also be constructed for the Slepian spatial-spectral concentration problem for the Fourier-Laguerre spectral domain.

Thus, the spectral representation \mathbf{f} of the band-limited spatially concentrated signal f can be obtained as a solution of an algebraic (finite dimensional) eigenvalue problem of size $PL^2 \times PL^2$. Due to the continuous nature of the Fourier-Bessel harmonic space (i.e. k is continuous), an equivalent finite-dimensional matrix formulation cannot be written for the Fourier-Bessel setting.

For the eigenvalue problems (36) and (42), which are expressed in terms of the spatial domain representation of the signal, we have obtained here the equivalent harmonic formulations (44) and (48) respectively. In the next section, we discuss the properties of band-limited and space-limited eigenfunctions.

3.5. Review

In the present section, we first formulated two types of eigenvalue problems: (1) problem (29) and (30) to find band-limited spatially concentrated functions f ; and (2) problems (33) and (34) to find space-limited functions g with optimal concentration within a spectral region. We then showed that the eigenfunctions that arise as a solution of both problems are the same, up to a multiplicative constant, within the spatial

region R and spectral region A_{PL} or \tilde{A}_{KL} . Due to the equivalence of the spatial and spectral concentration problems, we are only required to solve the eigenvalue problem presented in (36) (Fourier-Bessel domain) or (42) (Fourier-Laguerre domain) to obtain the band-limited spatially concentrated eigenfunctions. For these eigenvalue problems (36) and (42), which are expressed in terms of the spatial domain representation of the signal, we have also obtained the equivalent harmonic formulations (44) and (48) respectively. For the concentration problems for Fourier-Bessel spectral domain, we encapsulate the key developments presented in this section in the form of concept map presented in Fig. 1, where we have also summarised the key properties, presented in detail in the next section, of the band-limited and space-limited eigenfunctions. The equivalent concept map for the Fourier-Laguerre spectral domain is analogous.

4. Analysis of Eigenfunctions and Eigenvalue Spectrum

We first study the properties of the both band-limited and space-limited eigenfunctions in this section, both for the Fourier-Bessel and Fourier-Laguerre scenarios. In both of these scenarios we also study the eigenvalue spectrum and calculate the analog of the Shannon number in the one dimensional Slepian concentration problem.

4.1. Properties of Fourier-Bessel Band-Limited Eigenfunctions

The Fourier-Bessel band-limited and spatially concentrated eigenfunctions are recovered in the spectral domain by solving the eigenvalue problem given in (44). That is, we obtain $f_{\ell m}(k)$ for $0 \leq k \leq K$, $0 \leq \ell \leq L - 1$ and $|m| \leq \ell$. In practice [24, 23, 21], the spectrum along $k \in \mathbb{R}^+$ is discretized to solve the eigenvalue problem in (44) as an algebraic eigenvalue problem (we further elaborate this in Section 5). Since both (36) and (44) are equivalent and the operator U , with kernel given in (35), is a self-adjoint composition of projection operators, the eigenfunctions are orthogonal and the associated eigenvalue of each eigenfunction is real, positive and bounded above by unity. We choose the eigenfunctions to be orthonormal. Since the spectral response is continuous along k , the number of eigenfunctions is (theoretically) infinite and depends on the resolution of the discretization of the spectrum along k . We order eigenfunctions f^1, f^2, \dots and eigenvalues $\lambda_1, \lambda_2, \dots$ such that $1 > \lambda_1 \geq \lambda_2 \geq \dots > 0$.

The eigenfunctions $f^\alpha \in L^2(\mathbb{B}^3)$ in the spatial domain can be recovered from their spectral representation through the inverse Fourier-Bessel transform (13), where α is used to index the eigenfunctions. Since the Hermitian symmetry property $\mathcal{X}_{\ell m, \ell' m'}(k, k') = (\mathcal{X}_{\ell' m', \ell m}(k', k))^*$ is satisfied, as is directly apparent from (45), it follows that the eigenvalues are real and the eigenfunctions orthogonal. The band-limited eigenfunctions are orthonormal in both the Fourier-Bessel spectral domain and in the entire spatial domain

\mathbb{B}^3 , that is,

$$\sum_{\ell=0}^{L-1} \sum_{m=-\ell}^{\ell} \int_{\mathbb{R}^+} dk f_{\ell m}^{\alpha}(k) \left(f_{\ell m}^{\beta}(k) \right)^* = \delta_{\alpha\beta}, \quad (49)$$

$$\int_{\mathbb{B}^3} d^3\mu(\mathbf{r}) f^{\alpha}(\mathbf{r}) \left(f^{\beta}(\mathbf{r}) \right)^* = \delta_{\alpha\beta}. \quad (50)$$

The eigenfunctions are also orthogonal (but not orthonormal) within the spatial region R , with

$$\int_R d^3\mu(\mathbf{r}) f^{\alpha}(\mathbf{r}) \left(f^{\beta}(\mathbf{r}) \right)^* = \lambda_{\alpha} \delta_{\alpha\beta}, \quad (51)$$

which is obtained using the spectral domain formulation of the eigenvalue problem in (44) and the orthonormality relation in (49). It is clear from (51) that the eigenvalue λ associated with each unit energy band-limited eigenfunction provides a measure of energy concentration within the spatial region R .

4.2. Properties of Fourier-Laguerre Band-Limited Eigenfunctions

The Fourier-Laguerre band-limited and spatially concentrated eigenfunctions are recovered in the spectral domain by solving the eigenvalue problem given in (48), to recover the eigenvector \mathbf{f} . Since the matrix \mathcal{Z} in (48) is of size $PL^2 \times PL^2$, the number of eigenvectors/eigenfunctions is also PL^2 . The matrix \mathcal{Z} is positive definite, therefore the eigenvalues are positive, real and bounded by unity and the eigenvectors are orthogonal. We chose the eigenvectors to be orthonormal. We again order eigenvectors $\mathbf{f}^1, \mathbf{f}^2, \dots, \mathbf{f}^{PL^2}$ and eigenvalues $\lambda_1, \lambda_2, \dots, \lambda_{PL^2}$ such that $1 > \lambda_1 \geq \lambda_2 \geq \dots \geq \lambda_{PL^2} > 0$.

The eigenfunctions $f^{\alpha}(\mathbf{r})$ in the spatial domain can be recovered from their spectral representation through the inverse Fourier-Laguerre transform (16), where again α is used to index the eigenfunctions. Again, the reality of eigenvalues and orthogonality of eigenvectors also follows from the fact that the matrix \mathcal{Z} in (47), with entries given in (48), is Hermitian symmetric. The band-limited eigenfunctions are orthonormal in both the Fourier-Laguerre spectral domain and in the entire spatial domain \mathbb{B}^3 , that is,

$$\left(\mathbf{f}^{\alpha} \right)^H \mathbf{f}^{\beta} = \sum_{p=0}^{P-1} \sum_{\ell=0}^{L-1} \sum_{m=-\ell}^{\ell} \left(f_{\ell m p}^{\alpha} \right)^* f_{\ell m p}^{\beta} = \delta_{\alpha\beta}, \quad (52)$$

$$\int_{\mathbb{B}^3} d^3\mu(\mathbf{r}) f^{\alpha}(\mathbf{r}) \left(f^{\beta}(\mathbf{r}) \right)^* = \delta_{\alpha\beta}, \quad (53)$$

where $(\cdot)^H$ denotes the Hermitian transpose operation, and are orthogonal (but not orthonormal) within the spatial region R ,

$$\int_R d^3\mu(\mathbf{r}) f^{\alpha}(\mathbf{r}) \left(f^{\beta}(\mathbf{r}) \right)^* = \lambda_{\alpha} \delta_{\alpha\beta}, \quad (54)$$

which is obtained by using (46) and the orthonormality relation in (52). It is clear from (54) that the eigenvalue λ_{α} associated with each unit energy band-limited eigenfunction f^{α} provides a measure of energy concentration within the spatial region R .

4.3. Properties of Space-Limited Eigenfunctions

As highlighted earlier, the space-limited spectrally concentrated eigenfunctions $g(\mathbf{r})$ of the eigenvalue problems (33) and (34) can be obtained from the band-limited spatially concentrated eigenfunctions of problems (44) and (48), respectively. This is achieved by employing the relationship given in (41), i.e., by setting the space-limited eigenfunctions to the band-limited eigenfunctions in the region R and zero elsewhere.

Each band-limited eigenfunction $f^\alpha(\mathbf{r})$ thus provides a space-limited eigenfunction $g^\alpha(\mathbf{r})$ and the eigenvalue associated with each eigenfunction provides a measure of energy concentration within the Fourier-Bessel or Fourier-Laguerre spectral domain. In order to normalize the space-limited eigenfunctions to unit energy, we update the relationship between $f^\alpha(\mathbf{r})$ and $g^\alpha(\mathbf{r})$, given in (41), by noting (51) and (54), as

$$g^\alpha(\mathbf{r}) = \frac{1}{\sqrt{\lambda_\alpha}} (\mathcal{S}_R f^\alpha)(\mathbf{r}), \quad \lambda_\alpha \neq 0. \quad (55)$$

The revised space-limited eigenfunctions $g^\alpha(\mathbf{r})$ then satisfy

$$\int_{\mathbb{B}^3} d^3\mu(\mathbf{r}) g^\alpha(\mathbf{r}) (g^\beta(\mathbf{r}))^* = \int_R d^3\mu(\mathbf{r}) g^\alpha(\mathbf{r}) (g^\beta(\mathbf{r}))^* = \delta_{\alpha\beta}. \quad (56)$$

The relation between the band-limited eigenfunctions $f^\alpha(\mathbf{r})$ and space-limited eigenfunctions $g^\alpha(\mathbf{r})$ can be expressed in the spectral domain as

$$\begin{aligned} g_{\ell m}^\alpha(k) &= \frac{1}{\sqrt{\lambda_\alpha}} \sum_{\ell'=0}^{L-1} \sum_{m'=-\ell}^{\ell} \int_{k'=0}^K dk' \mathcal{X}_{\ell' m', \ell m}(k', k) f_{\ell' m'}^\alpha(k'), \quad f^\alpha(\mathbf{r}) \in \tilde{\mathcal{H}}_{KL}, \\ g_{\ell m p}^\alpha &= \frac{1}{\sqrt{\lambda_\alpha}} \sum_{p'=0}^P \sum_{\ell'=0}^{L-1} \sum_{m'=-\ell'}^{\ell'} \mathcal{Z}_{\ell' m' p', \ell m p} f_{\ell' m' p'}^\alpha, \quad f^\alpha(\mathbf{r}) \in \mathcal{H}_{PL}, \end{aligned} \quad (57)$$

for $\ell, p \in \mathbb{Z}^+$ and $k \in \mathbb{R}^+$, where we have used the kernel representation of the spatial-selection operator \mathcal{S}_R . Note that the harmonic representations of the space-limited eigenfunctions $g_{\ell m}^\alpha(k)$ and $g_{\ell m p}^\alpha$ are obviously not band-limited and the expressions given above apply over the entire harmonic domains. Using (44) and (46) these relations can also be expressed within the finite spectral regions as

$$\begin{aligned} g_{\ell m}^\alpha(k) &= \sqrt{\lambda_\alpha} f_{\ell m}^\alpha(k), \quad \ell, k \in \tilde{A}_{KL}, \\ g_{\ell m p}^\alpha &= \sqrt{\lambda_\alpha} f_{\ell m p}^\alpha, \quad \ell, p \in A_{PL}. \end{aligned} \quad (58)$$

Finally, using (49) or (52) in conjunction with (58), we can obtain the orthogonality relations for space-limited eigenfunctions in the spectral domain

$$\begin{aligned} \sum_{\ell=0}^{L-1} \sum_{m=-\ell}^{\ell} \int_{k=0}^K dk g_{\ell m}^\alpha(k) (g_{\ell m}^\beta(k))^* &= \lambda_\alpha \delta_{\alpha\beta}, \\ \sum_{p=0}^{P-1} \sum_{\ell=0}^{L-1} \sum_{m=-\ell}^{\ell} g_{\ell m p}^\alpha (g_{\ell m p}^\beta)^* &= \lambda_\alpha \delta_{\alpha\beta}. \end{aligned} \quad (59)$$

It is clear from (59) that the eigenvalue λ associated with each unit energy space-limited eigenfunction provides a measure of energy concentration within the spectral regions \tilde{A}_{KL} or A_{PL} .

Remark 2. *We highlight again that the eigenvalue λ_α serves as a measure of the concentration of the (unit energy) band-limited eigenfunctions $f^\alpha(\mathbf{r})$ in the spatial domain, and the concentration of the (unit energy) space-limited eigenfunctions $g^\alpha(\mathbf{r})$ in the spectral domain. The energy $1 - \lambda_\alpha$ leaked by $f^\alpha(\mathbf{r})$ into the spatial region $\mathbb{B}^3 \setminus R$ is equal to the energy leaked by $g^\alpha(\mathbf{r})$ outside of the spectral region \tilde{A}_{KL} or A_{PL} , depending on the chosen spectral domain.*

Remark 3. *Since \mathcal{H}_R is an infinite dimensional subspace of $L^2(\mathbb{B}^3)$, the number of space-limited eigenfunctions arising from the solution of (34) is infinite. However, when we maximize the spatial concentration of the functions band-limited in the Fourier-Laguerre spectral domain, the equivalent problem in the spectral domain given in (48) is finite dimensional, giving rise to a finite number (PL^2) of band-limited, and thus also space-limited, eigenfunctions. The remaining space-limited eigenfunctions, which do not have any energy in the spatial region R nor in the spectral region A_{PL} , belong to the infinite dimensional null space of (34) and have associated eigenvalue equal to zero.*

4.4. Eigenvalue Spectrum

Following Remark 2, the band-limited eigenfunctions and space-limited eigenfunctions, which are well concentrated within the spatial region and spectral region respectively, have eigenvalue near unity, whereas those which are poorly concentrated have value near zero. If the spectrum of eigenvalues $\lambda_1, \lambda_2, \dots$, has a narrow transition width from values near unity to values near zero, as in the case of one dimensional Slepian concentration problem [43] and spherical concentration problem [36], the sum of all of the eigenvalues well approximates the number of significant eigenfunctions with eigenvalue near unity. We elaborate this fact later in the paper with the help of examples. If the signal is band-limited in the Fourier-Bessel spectral domain, the sum of eigenvalues is given by

$$\begin{aligned} \tilde{N}_{KL} = \text{tr}(\mathbf{U}) &= \int_{\mathbb{B}^3} d^3\mu(\mathbf{r}) U(\mathbf{r}, \mathbf{r}) = \int_{k=0}^K dk \sum_{\ell=0}^{L-1} \sum_{m=-\ell}^{\ell} \mathcal{X}_{\ell m, \ell m}(k, k) \\ &= \sum_{\ell=0}^{L-1} \frac{2\ell+1}{2\pi^2} \int_R d^3\mu(\mathbf{r}) \left(\int_{k=0}^K dk k^2 j_\ell(kr) j_\ell(kr) \right) \\ &= \sum_{\ell=0}^{L-1} \frac{2\ell+1}{4\pi^2} K^3 \int_R d^3\mu(\mathbf{r}) \left((j_\ell(Kr))^2 - j_{\ell-1}(Kr) j_{\ell+1}(Kr) \right), \end{aligned} \quad (60)$$

with $\mathbf{r} = \mathbf{r}(r, \theta, \phi)$. Here we use $\text{tr}(\cdot)$ to denote the trace of an operator or a matrix.

For a signal band-limited in the Fourier-Laguerre spectral domain, the sum of eigenvalues is given by

$$\begin{aligned}
N_{PL} &= \text{tr}(\mathbf{W}) = \text{tr}(\mathbf{Z}) = \int_{\mathbb{B}^3} d^3\mu(\mathbf{r})W(\mathbf{r}, \mathbf{r}) \\
&= \sum_{p=0}^{P-1} \sum_{\ell=0}^{L-1} \sum_{m=-\ell}^{\ell} Z_{\ell mp, \ell mp} \\
&= \frac{L^2}{4\pi} \sum_{p=0}^{P-1} \int_R d^3\mu(\mathbf{r})K_p(r)K_p(r), \quad \mathbf{r} = \mathbf{r}(r, \theta, \phi).
\end{aligned} \tag{61}$$

We note that the sum of eigenvalues given in (60) and (61) involve an integral of a positive function over the spatial region R . Thus, if the volume of the spatial region is relatively smaller, the sum of eigenvalues, which also indicates the number of significant eigenfunctions, is also smaller.

Remark 4. \tilde{N}_{KL} and N_{PL} serve as an analog of the Shannon number in the one-dimensional Euclidean Slepian concentration problem [43, 31], in which the Shannon number is given by a space-bandwidth product. Here, we refer to N_{KL} or N_{PL} as spherical Shannon numbers. Since the significant eigenfunctions have value near unity and the remaining eigenfunctions have eigenvalue near zero, the number of significant eigenfunctions is given approximately by \tilde{N}_{KL} or N_{PL} . Thus, a function spatially concentrated in R and band-limited in the Fourier-Bessel (Fourier-Laguerre) domain within the spectral region \tilde{A}_{KL} (A_{PL}), can be represented approximately by \tilde{N}_{KL} (N_{PL}) band-limited orthonormal eigenfunctions. This is the essence of the concentration problem: spatially concentrated band-limited functions on the ball, which belong to the infinite dimensional space $\tilde{\mathcal{H}}_{KL}$, can be approximately represented by \tilde{N}_{KL} finite orthonormal basis functions of the same space. Similarly, the dimension of the space required to represent spatially concentrated band-limited signals belonging to the finite dimensional space $\tilde{\mathcal{H}}_{KL}$ of size PL^2 can be reduced from PL^2 to N_{PL} . This fact is further explored in Section 6.

Remark 5. The approximation of the number of significant eigenfunctions by the spherical Shannon number \tilde{N}_{KL} or N_{PL} is based on an assumption that the spectrum of eigenvalues has a narrow transition width from values near unity to values near zero. This assumption can be further studied by computing the Hilbert-Schmidt norm of the integral operators \mathbf{U} or \mathbf{W} . Since the Hilbert-Schmidt norm is equal to the sum of the squares of the eigenvalues, the difference between the Hilbert-Schmidt norm and the spherical Shannon number can be used as a measure to quantify the transition width of the spectrum of eigenvalues. Since we actually compute the eigenvalues (later in the paper), we do not carry out further analysis to determine the transition width of the eigenvalues spectrum and the distribution of the eigenvalues (e.g., [17, 20]) using the Hilbert-Schmidt of the operator defining the eigenvalue problem.

5. Eigenfunctions Concentrated within Spatially Symmetric Regions

In the preceding section we analysed the properties of eigenfunctions arising from the spatial-spectral concentration problem on the ball. We have yet to discuss the computation of these eigenfunctions. As mentioned briefly earlier, the eigenvalue problem of (44) to find eigenfunctions band-limited in the Fourier-Bessel domain can be transformed into an algebraic eigenvalue problem by discretizing the spectrum along $k \in \mathbb{R}^+$. If we discretize along k with a step size Δk by selecting $M \triangleq \lceil K/\Delta k \rceil$ uniform samples $k_n = nK/M, n = 1, 2, \dots, M$, between $0 < k \leq K$, the eigenvalue problem in (44) becomes an algebraic eigenvalue problem of size ML^2 , for which we need to compute a Hermitian matrix of size $ML^2 \times ML^2$. For each element of this matrix we must evaluate the integral given in (45) over the spatial region of interest. Similarly, the eigenvalue problem of (46), of size PL^2 , must be solved to find band-limited eigenfunctions in the Fourier-Laguerre domain. Again, for each element of the matrix we must evaluate the integral given in (47) over the spatial region of interest. Since observations in practical applications can support very high band-limits, the direct computation of eigenfunctions by solving the algebraic eigenvalue problems is computationally intensive, motivating alternative procedures.

In this section we analyze the eigenvalue problems when the spatial region of concentration is symmetric in nature. Under certain symmetries we show that the eigenvalue problems given in the spectral domain in (44) and (48), originally formulated in (36) and (42), decompose into subproblems, which reduce the computational burden. In some special cases $\mathcal{X}_{\ell m, \ell' m'}(k, k')$ in (45) and $\mathcal{Z}_{\ell m p, \ell' m' p'}$ in (47) can be computed analytically. We consider two types of symmetric regions: (1) circularly symmetric regions only; and (2) circularly symmetric and radially independent regions, which are formally defined below:

Definition 4 (Circularly Symmetric Region). *We define a region to be circularly symmetric if it is rotationally symmetric around some rotation axis defined by its center $\mathbf{r}_0 \triangleq \mathbf{r}_0(r_0, \theta_0, \phi_0) \in \mathbb{B}^3$.*

Definition 5 (Circularly Symmetric and Radially Independent Region). *In addition to circular symmetry, if the spatial region R is also radially independent, that is, $R = R_s \times R_r$ with $R_s \subset \mathbb{S}^2$ and $R_r \subset \mathbb{R}^+$, the region is referred to as circularly symmetric and radially independent region.*

5.1. Circularly Symmetric Region Only

First, we analyze the case when the spatial region is circularly symmetric. For convenience, we consider the region with rotation axis $\boldsymbol{\eta}_0 \triangleq \boldsymbol{\eta}_0(r_0, 0, 0) \in \mathbb{B}^3$ on the z -axis and refer to such a region as an azimuthally symmetric region. Through a rotation of θ_0 around the y -axis, followed by a rotation of ϕ_0 around the z -axis, the azimuthally symmetric region with center at $\boldsymbol{\eta}_0$ can be transformed into the circularly symmetric region with center at \mathbf{r}_0 . When considering the azimuthally symmetric region, the azimuthal angle becomes independent of r and θ and therefore we can write the integral over region R as $\int_R \equiv \int_{(r, \theta)} \int_{\phi=0}^{2\pi}$. Noting this

decoupling of the integral and the orthonormality of the complex exponentials, we can simplify $\mathcal{X}_{\ell m, \ell' m'}(k, k')$ given in (45) as

$$\begin{aligned}\mathcal{X}_{\ell m, \ell' m'}(k, k') &= \delta_{mm'} 2\pi \int_{(r, \theta)} r^2 \sin \theta dr d\theta X_{\ell m}(k, \mathbf{r}) X_{\ell' m'}^*(k', \mathbf{r}), \quad \mathbf{r} = \mathbf{r}(r, \theta, 0) \\ &= \delta_{mm'} \mathcal{X}_{\ell m, \ell' m}(k, k'),\end{aligned}\tag{62}$$

which can be used to decompose the spectral domain eigenvalue problem in (44) into $2L - 1$ subproblems,

$$\int_{k'=0}^K dk' \sum_{\ell'=0}^{L-1} \mathcal{X}_{\ell' m, \ell m}(k', k) f_{\ell' m}(k') = f_{\ell m}(k),\tag{63}$$

for each $m \in \{-(L-1), \dots, (L-1)\}$. Furthermore, it can be easily shown that $\mathcal{X}_{\ell m, \ell' m}(k, k') = \mathcal{X}_{\ell(-m), \ell'(-m)}(k, k')$ which leaves us with L subproblems for $m \in \{0, 1, \dots, (L-1)\}$. The subproblem in (63) gives the spectral domain representation $f_{\ell m}(k)$ of eigenfunctions for each m , which can be used to obtain the spatial functions for each m as

$$f^{(m)}(r, \theta) = \int_{k=0}^K dk \sum_{\ell=m}^{L-1} f_{\ell m}(k) X_{\ell m}(k, \mathbf{r}), \quad \mathbf{r} = \mathbf{r}(r, \theta, 0).\tag{64}$$

Furthermore, since $\mathcal{X}_{\ell' m, \ell m}(k', k) = \mathcal{X}_{\ell m, \ell' m}(k, k')$ is real valued, the spectral domain representation $f_{\ell m}(k)$ of the eigenfunction and consequently the spatial eigenfunction $f^{(m)}(r, \theta)$ is real valued. We note that the superscript m on the left hand side of (64) indicates angular order and should not be confused with the rank of the eigenfunction.

Similarly, the symmetry of the region along the z -axis also simplifies the elements $\mathcal{Z}_{\ell m p, \ell' m' p'}$ in (47) as

$$\mathcal{Z}_{\ell m p, \ell' m' p'} = \delta_{mm'} \mathcal{Z}_{\ell m p, \ell' m p'} = \delta_{(-m)(-m')} \mathcal{Z}_{\ell(-m) p, \ell'(-m) p'},\tag{65}$$

due to which the matrix \mathcal{Z} becomes block diagonal. By defining the matrix $\mathcal{Z}^{(m)}$ of size $P(L-m) \times P(L-m)$, with entries

$$\mathcal{Z}_{\ell p, \ell' p'}^{(m)} = \mathcal{Z}_{\ell m p, \ell' m p'},\tag{66}$$

the matrix eigenvalue problem in (48) can be decomposed into L subproblems of the following form

$$\mathcal{Z}^{(m)} \mathbf{f}^{(m)} = \lambda \mathbf{f}^{(m)},\tag{67}$$

for each $m \in \{0, 1, \dots, L-1\}$. The vector $\mathbf{f}^{(m)} \triangleq (f_{mm0}, f_{mm1}, \dots, f_{mm(P-1)}, \dots, f_{(L-1)(m)(P-1)})^T$ of length $P(L-m)$ represents the spectral domain response of the band-limited eigenfunction for given order m , given by

$$f^{(m)}(r, \theta) = \sum_{p=0}^{P-1} \sum_{\ell=m}^{L-1} f_{\ell m p} \mathcal{Z}_{\ell m p}(r, \theta, 0).\tag{68}$$

Again, due to the fact that the matrix $\mathcal{Z}^{(m)}$ is real valued and symmetric, both $\mathbf{f}^{(m)}$ and $f^{(m)}(r, \theta)$ are real valued.

Using the spatial domain eigenfunction $f^{(m)}(r, \theta)$ for each m given by (64) and (68), the eigenfunction $f(\mathbf{r})$ can be obtained by scaling with the complex exponential $e^{im\phi}$, characterizing the variation of an eigenfunction along azimuth, giving

$$f(\mathbf{r}) = f^{(m)}(r, \theta)e^{im\phi} = \sum_{p=0}^{P-1} \sum_{\ell=m}^{L-1} f_{\ell mp} Z_{\ell mp}(r, \theta, \phi), \quad \mathbf{r} = \mathbf{r}(r, \theta, \phi). \quad (69)$$

To summarise this subsection, the symmetry of the spatial region along azimuth allows the decomposition of the large eigenvalue problem that includes all angular orders $-(L-1) \leq m \leq L-1$ into smaller L subproblems, each for single angular order $m \in \{0, 1, 2, \dots, L-1\}$.

5.2. Circularly Symmetric and Radially Independent Region

In the previous subsection, we showed that the eigenvalue problem decomposes into subproblems for circularly symmetric regions. For circularly symmetric and radially independent regions, the eigenvalue problem decomposes further into subproblems. For convenience, we again consider a circularly symmetric and radially independent region defined as

$$R \triangleq \{R_1 \leq r \leq R_2, \theta_1 \leq \theta \leq \theta_2, 0 \leq \phi < 2\pi\}, \quad (70)$$

which is circularly symmetric around rotation axis $\boldsymbol{\eta}_0 \triangleq \boldsymbol{\eta}_0(r_0, 0, 0) \in \mathbb{B}^3$ on the z -axis. Note that the region R , given in (70), becomes a spherical shell region, characterized by R_1 and R_2 , for $\theta_1 = 0$ and $\theta_2 = \pi$, which reduces to a spherical symmetric (volume) region of radius R_2 for $R_1 = 0$.

For the circularly symmetric and radially independent region R given in (70), the integral over the spatial region R decouples as $\int_R \equiv \int_{r=R_1}^{R_2} \int_{\theta=\theta_1}^{\theta_2} \int_{\phi=0}^{2\pi}$, which can be incorporated to simplify $\mathcal{X}_{\ell m, \ell' m'}(k, k')$ given in (62) as

$$\begin{aligned} \mathcal{X}_{\ell m, \ell' m'}(k, k') &= \delta_{mm'} \underbrace{\frac{2}{\pi} \int_{r=R_1}^{R_2} r^2 dr k k' j_\ell(kr) j'_\ell(k'r)}_{C_{\ell, \ell'}(k, k')} \\ &\times \underbrace{2\pi \int_{\theta=\theta_1}^{\theta_2} \sin \theta d\theta Y_{\ell m}(\theta, 0) Y_{\ell' m}^*(\theta, 0)}_{G_{\ell, \ell'}^m}. \end{aligned} \quad (71)$$

The integral $C_{\ell, \ell'}(k, k')$ can be evaluated analytically for some special cases. When $k = k'$,

$$C_{\ell, \ell'}(k, k) = k^{2+\ell+\ell'} 2^{(-2-\ell-\ell')} \Gamma(2+\ell+\ell') (F_1(\ell, \ell', kR_2) - F_1(\ell, \ell', kR_1)), \quad (72)$$

where

$$F_1(\ell, \ell', kR) = R^{3+\ell+\ell'} {}_pF^q \left(\left[\frac{2+\ell+\ell'}{2}, \frac{3+\ell+\ell'}{2}, \frac{3+\ell+\ell'}{2} \right], \dots \right. \\ \left. \dots \left[\frac{3+2\ell}{2}, \frac{5+\ell+\ell'}{2}, \frac{3+2\ell'}{2}, 2+\ell+\ell' \right], -k^2 R^2 \right) \quad (73)$$

is the Hypergeometric generalized regularized function.⁴ When $\ell = \ell'$,

$$C_{\ell,\ell}(k, k') = \begin{cases} \frac{2\sqrt{kk'}}{\pi(k^2-k'^2)} \left(R_2^2 k' j_{\ell-1}(k' R_2) j_{\ell}(k R_2) - R_2^2 k j_{\ell-1}(k R_2) j_{\ell}(k' R_2) \right. \\ \left. - R_1^2 k' j_{\ell-1}(k' R_1) j_{\ell}(k R_1) + R_1^2 k j_{\ell-1}(k R_1) j_{\ell}(k' R_1) \right) & k \neq k' \\ \frac{k}{2\pi} (T(\ell, k, R_2) - T(\ell, k, R_2)) & k = k' \end{cases} \quad (74)$$

with $T(\ell, k, R_1) = R_1^3 (j_{\ell}^2(k R_1) - j_{\ell-1}(k R_1) j_{\ell+1}(k R_1))$. The integral $G_{\ell,\ell'}^m$ can be evaluated analytically for all $\ell, \ell' \geq |m|$ by [36]

$$G_{\ell,\ell'}^m = (-1)^m \frac{\sqrt{(2\ell+1)(2\ell'+1)}}{2} \sum_{j=|\ell-\ell'|}^{|\ell+\ell'|} \begin{pmatrix} \ell & j & \ell' \\ 0 & 0 & 0 \end{pmatrix} \begin{pmatrix} \ell & j & \ell' \\ m & 0 & -m \end{pmatrix} \\ \times (P_{j-1}^0(\cos \theta_2) + P_{j+1}^0(\cos \theta_1) - P_{j+1}^0(\cos \theta_2) - P_{j-1}^0(\cos \theta_1)), \quad (75)$$

where the arrays of indices are Wigner-3j symbols [33]. We note that the integral $C_{\ell,\ell'}(k, k')$ depends on only R_1 and R_2 , and the integral denoted by $G_{\ell,\ell'}^m$ depends on only θ_1 and θ_2 . For brevity, this dependence is not explicit in the notation. The azimuthal symmetry of the spatial region allows the eigenvalue problem to be decomposed into sub-problems and the independence between r and θ enables the analytic computation of $\mathcal{X}_{\ell m, \ell' m'}(k, k')$ when $\ell = \ell'$ or $k = k'$. For the Fourier-Bessel setting, the independence between r and θ in the definition of the region does not allow further decomposition of the problem due to the coupling between the radial and angular spectral components, characterized by, respectively, the Bessel functions $j_{\ell}(kr)$ and the spherical harmonics $Y_{\ell m}(\theta, \phi)$ (i.e., the harmonic index ℓ is shared).

For the Fourier-Laguerre setting, the independence between the radial component r and angular colatitude θ allows us to further decompose the eigenvalue problem given in (67) since the radial and angular spectral domains are also decoupled. Considering the azimuthally and radially symmetric region R , the elements of the matrix \mathcal{Z}^m given in (66) can be expressed as

$$\mathcal{Z}_{\ell p, \ell' p'}^m = \underbrace{\int_{r=R_1}^{R_2} r^2 dr K_p(r) K_{p'}(r)}_{E_{p,p'}} \underbrace{2\pi \int_{\theta=\theta_1}^{\theta_2} \sin \theta d\theta Y_{\ell m}(\theta, 0) Y_{\ell' m}^*(\theta, 0)}_{G_{\ell,\ell'}^m}. \quad (76)$$

Since there is no dependence between the integrals along the radial and angular spectral components, the

⁴Mathematica: HypergeometricPFQRegularized

fixed order eigenvalue problem in (67) can be decomposed into two separate eigenvalue subproblems:

$$\sum_{p'=0}^{P-1} E_{p',p} f_{p'} = \lambda^1 f_p, \quad f \in L^2(\mathbb{R}^+), \quad (77)$$

$$\sum_{\ell'=m}^{L-1} G_{\ell',\ell}^m f_{\ell'm} = \lambda^2 f_{\ell m}, \quad f \in L^2(\mathbb{S}^2). \quad (78)$$

The eigenvalue problem in (77) maximizes the concentration of the band-limited signal defined on \mathbb{R}^+ in the interval $r \in [R_1, R_2]$ and the eigenvalue problem in (78) maximizes the concentration of the signal defined on \mathbb{S}^2 in the region characterized by colatitude $\theta \in [\theta_1, \theta_2]$. We note that the eigenvalue problem in (77) is independent of angular order m and is an algebraic eigenvalue problem of size P , therefore its solution provides the spectral domain representation of P orthonormal eigenfunctions defined on \mathbb{R}^+ . The sum of eigenvalues is given by

$$N^P = \sum_{p=0}^{P-1} E_{p,p}, \quad (79)$$

which also indicates the number of significant eigenfunctions with eigenvalues near unity. An analytic expression to evaluate $E_{p,p'}$ can be obtained by using the definition of the Laguerre basis functions in (6) and (7), yielding

$$E_{p,p'} = \sqrt{\frac{p! p'!}{(p+2)!(p'+2)!}} e^{-r} \sum_{j=0}^p \sum_{j'=0}^{p'} \frac{(-1)^{j+j'}}{j! j'!} \binom{p+2}{p-j} \binom{p'+2}{p'-j'} \times \int dr e^{-r} r^{j+j'+2}, \quad (80)$$

where the integral can be evaluated using the upper incomplete gamma function [4] as

$$\int dr e^{-r} r^{j+j'+2} = (j+j'+2)! \sum_{a=0}^{j+j'+2} \frac{e^{-R_1} (R_1)^a - e^{-R_2} (R_2)^a}{a!}. \quad (81)$$

Similarly, the solution of the eigenvalue problem in (78) for each m gives rise to $L - m$ eigenfunctions defined on \mathbb{S}^2 . The sum of eigenvalues for all orders is given by

$$N_L = \sum_{m=-(L-1)}^{L-1} \sum_{\ell=|m|}^{L-1} G_{\ell,\ell}^m = \frac{L^2}{2} (\cos \theta_1 - \cos \theta_2). \quad (82)$$

Explicit expressions to determine the sum of eigenvalues for each order m have been derived in [36], where the subproblem in (78) to find band-limited functions on the sphere with optimal spatial concentration in the polar cap region about the North pole has been investigated in detail. By the decompositions due to the symmetry of the region, the spherical Shannon number in (61) can be expressed as

$$N_{PL} = N^P N_L. \quad (83)$$

For the Fourier-Laguerre setting, the band-limited eigenfunction $f^{(m)}(r, \theta)$ given by the solution of the fixed order eigenvalue problem in (67) can be expressed in terms of the solution of the subproblems given in (77) and (78) as

$$f^{(m)}(r, \theta) = \sum_{p=0}^{P-1} \sum_{\ell=m}^{L-1} f_p f_{\ell m} Z_{\ell m p}(r, \theta, 0), \quad (84)$$

where the eigenvalue $\lambda = \lambda^1 \lambda^2$ is a measure of concentration in the spatial region R . The band-limited eigenfunction $f(\mathbf{r})$ can be obtained by scaling $f^{(m)}(r, \theta)$ with the complex exponential $e^{im\phi}$, as given in (69).

Remark 6. *If the region $R \subset \mathbb{B}^3$ is not circularly symmetric but is radially independent, that is, $R = R_s \times R_r$, then due to the separability of the Fourier-Laguerre functions, the eigenvalue problem in the Fourier-Laguerre domain formulated in (48) can be decomposed into subproblems to separately find band-limited functions in the region R_r as formulated in (77) and in the region R_s as formulated in [36]. Using (61) in conjunction with (79), the spherical Shannon number for a radially independent region $R = R_s \times R_r$ is given by*

$$N_{PL} = \frac{N^P L^2}{4\pi} \int_{R_s} d^2\nu(\hat{\mathbf{r}}). \quad (85)$$

It must be noted that no simplification is possible for the problem in the Fourier-Bessel domain, formulated in (44), due to the spectral coupling between the radial and angular components in the Fourier-Bessel functions.

Remark 7. *Unlike the eigenvalue problem to find band-limited eigenfunctions in the Fourier-Bessel domain, the separation of the integrals over the spatial region due to the independence between r and θ completely decouples the problem to find band-limited eigenfunctions in the Fourier-Laguerre domain, such that the eigenfunctions can be independently concentrated along radial component and angular component. Due to such decoupling, the eigenfunctions can be computed efficiently compared to the case when the spatial region does not exhibit symmetry and/or independence.*

Remark 8. *If one is interested in computing eigenfunctions in an arbitrarily spatial region, the region can be approximated by the union of T subregions $R = R_1 \cup R_2 \cup \dots \cup R_T$ such that each subregion is azimuthally symmetric and radially independent. Furthermore, as indicated earlier, an azimuthally symmetric region can be rotated to a circularly symmetric region. The rotation of eigenfunctions can be performed in the spectral domain through the use of Wigner-D functions [16, 33]. The decomposition of arbitrary spatial regions into symmetric (and rotated) subregions can be useful in two respects. First, entries of the matrix defining an algebraic eigenvalue problem can be efficiently computed due to the separation of integrals and spectral decoupling (Remark 7). Second, the eigenvalue problem of larger size may be decomposed into a series of subproblems of smaller size provided the interactions between the subproblems are low-rank.*

5.3. Computational Considerations

In order to obtain band-limited eigenfunctions with spatial concentration in circularly symmetric and/or radially independent regions, we are required to solve algebraic eigenvalue problems formulated in (63) for discretized Fourier-Bessel spectral domain and (67), (77) and (78) for Fourier-Laguerre spectral domain. For some cases, we have derived analytic expressions to compute the entries of the matrix defining the eigenvalue problem that is required to be numerically diagonalized in order to obtain the band-limited eigenfunctions. In all of these cases, the entries of these matrices may also be obtained by adopting numerical quadrature to evaluate the defining integral. The Gauss-Legendre quadrature or equiangular sampling quadrature [26] can be used for discretization on \mathbb{S}^2 . For the discretization along $r \in \mathbb{R}^+$, the quadrature rules associated with the spherical Bessel transform and spherical Laguerre transform polynomials can be adopted⁵ [22]. The order of the quadrature, both on \mathbb{S}^2 and \mathbb{R}^+ , should be adjusted upward until the band-limited eigenfunctions satisfy the orthogonality relations, given in (49)–(51) or (52)–(54), to within machine precision or the desired level of accuracy. Note that the orthogonality relations are also evaluated using the same high order quadrature. The numerical quadrature is also applicable if the spatial region is of arbitrary shape and does not exhibit any symmetry. For such a spatial region, the lack of symmetry does not allow decomposition of the eigenvalue problem into subproblems, due to which we are required to solve an algebraic eigenvalue problem of size ML^2 or PL^2 , and therefore the computation of eigenfunctions may only be feasible for small-to-moderate band-limits.

Another computational consideration is the choice of step size Δk used for the discretization of the spectrum along $k \in \mathbb{R}^+$, which transforms the eigenvalue problem of (44) to find eigenfunctions band-limited in the Fourier-Bessel domain into an algebraic eigenvalue problem. In order to choose the step size Δk , we propose to take into account the following considerations: (1) Δk should be sufficiently small such that none of the eigenvalues $\lambda_1, \lambda_2, \dots$, are greater than unity; and (2) Δk should be small enough that the sum of eigenvalues is sufficiently close to the spherical Shannon number \tilde{N}_{KL} given in (60). The second consideration in choosing the step size Δk ensures that the further decrease in Δk does not result in the increase in the number of significant eigenfunctions (with eigenvalues near unity). This is the essence of the Slepian concentration problem: the infinite dimensional space $\tilde{\mathcal{H}}_{KL}$ is (approximately) spanned by \tilde{N}_{KL} finite orthonormal basis functions of the same space. In the next subsection, we illustrate that the sum of eigenvalues converges to the spherical Shannon number \tilde{N}_{KL} as $\Delta k \rightarrow 0$.

5.4. Illustration

As an example, we compute band-limited and space-limited eigenfunctions for the azimuthally and radially symmetric spatial region $R = \{15 \leq r \leq 25, \pi/8 \leq \theta \leq 3\pi/8, 0 \leq \phi < 2\pi\}$ and spectral regions

⁵Note that the evaluation of the quadrature (over the full spatial domain) is approximate and exact for the spherical Bessel transform and spherical Laguerre transform, respectively.

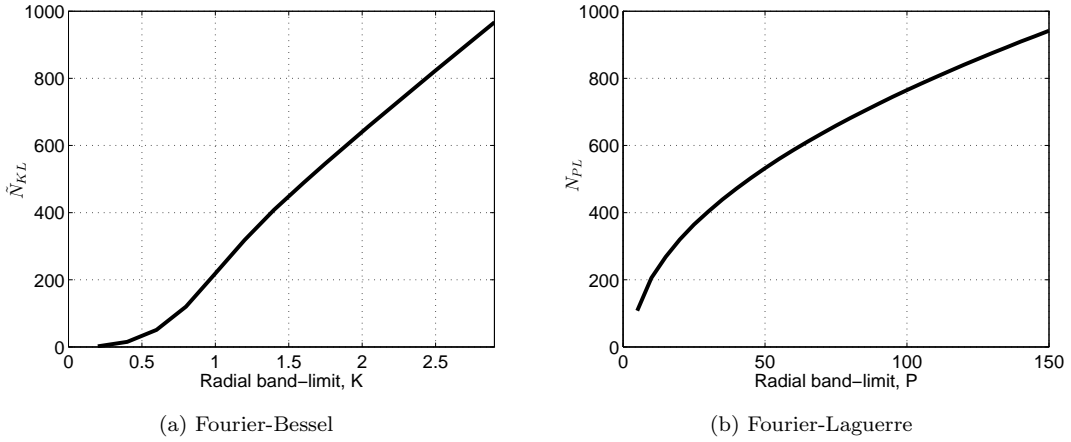


Figure 2: **Analytical plots for the spherical Shannon number** for (a) \tilde{N}_{KL} given in (60) for different values of band-limit K and (b) N_{PL} given in (61) for different values of band-limit P . The angular band-limit is $L = 20$ and the spatial region of concentration is $R = \{15 \leq r \leq 25, \pi/8 \leq \theta \leq 3\pi/8, 0 \leq \phi < 2\pi\}$.

$\tilde{A}_{KL} = \tilde{A}_{(1.4,20)}$ in the Fourier-Bessel spectral domain and $A_{PL} = A_{(30,20)}$ in the Fourier-Laguerre spectral domain. The band-limit $K = 1.4$ for the Fourier-Bessel domain is chosen such that, for the spatial region under consideration, the spherical Shannon numbers \tilde{N}_{KL} given in (60) and N_{PL} given in (61) are the same, i.e. $\tilde{N}_{KL} \approx N_{PL}$. The spherical Shannon numbers for this region are plotted in Fig. 2a and b respectively for different values of band-limits K and P . Since the region is azimuthally symmetric, the eigenfunctions band-limited in Fourier-Bessel and Fourier-Laguerre spectral domains can be found by solving the fixed-order eigenvalue problems formulated in (63) and (67) respectively.

For the computation of band-limited functions in the Fourier-Bessel domain, we discretize the spectrum along k with a step size of Δk . Due to the discretization of the spectrum along k , the problem in (63) reduces to a finite dimensional algebraic eigenvalue problem, the solution of which gives $L^2 K / \Delta k$ number of band-limited eigenfunctions. We analyse the effect of choosing different step sizes for the discretization of the spectrum along k . We plot the sum of eigenvalues and the spectrum of eigenvalues for different values of the step size $0.001 \leq \Delta k \leq 0.16$ in Fig. 3a and Fig. 3b respectively. It is evident in Fig. 3a that the sum of eigenvalues converges to the spherical Shannon number \tilde{N}_{KL} computed using the analytic expression (60). It is also worth noting from Fig. 3b that that the number of significant eigenfunctions is independent of the choice of discretization along k and thus confirms that the infinite dimensional subspace $\tilde{\mathcal{H}}_{KL}$ is, in fact, sufficiently spanned by the finite \tilde{N}_{KL} eigenfunctions. For the remaining of the illustration, we keep the step size $\Delta k = 0.02$, for which \tilde{N}_{KL} is greater than 99.9% of the sum of eigenvalues.

In order to find band-limited eigenfunctions in the Fourier-Laguerre domain as a solution of (67), we use the decomposition into the two subproblems formulated in (77) and (78) to separately maximize the radial and angular concentration respectively. From the band-limited eigenfunction f , the space-limited

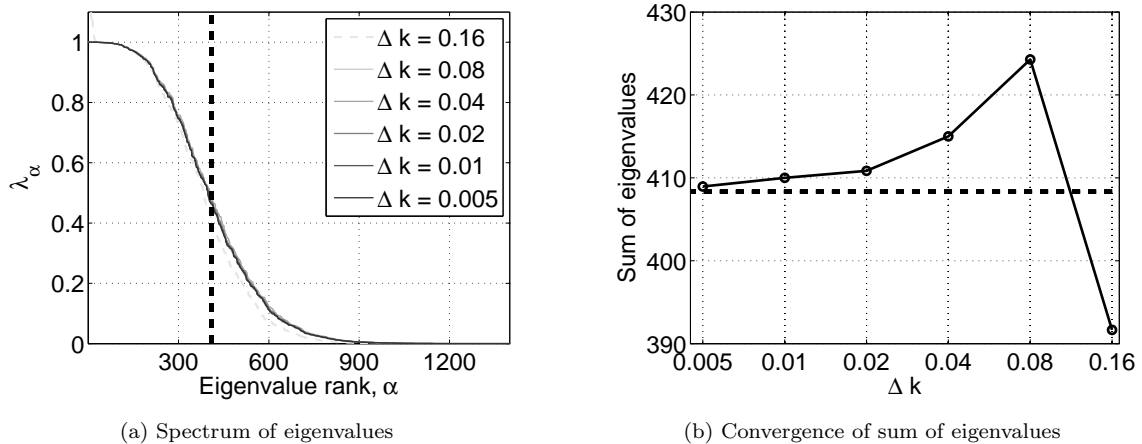


Figure 3: **Spectrum of eigenvalues for the Fourier-Bessel domain eigenvalue problem** formulated in (44) to find spatially concentrated eigenfunctions band-limited in the Fourier-Bessel domain in the spectral region $\tilde{A}_{(1.4,20)}$ and spatially concentrated in the region $R = \{15 \leq r \leq 25, \pi/8 \leq \theta \leq 3\pi/8, 0 \leq \phi < 2\pi\}$. For different step size $0.001 \leq \Delta k \leq 0.16$ used for the discretization of the spectrum along k , the spectrum of eigenvalues is plotted in (a) and the sum of eigenvalues is plotted in (b). The sum of eigenvalues, given by the spherical Shannon number $\tilde{N}_{KL} = 408.33$ (computed using analytic expression (60)) is also indicated by the straight dashed lines. The sum of eigenvalues converges to the spherical Shannon number in (b) as step size $\Delta k \rightarrow 0$. It can also be noted in (a) that the spherical Shannon number estimates the location of the transition in the eigenvalue spectrum accurately.

eigenfunction g can be obtained by limiting the band-limited eigenfunction f in the spatial domain using (55). Alternatively, the space-limited eigenfunction g can be obtained in the spectral domain from the band-limited eigenfunction f using (57). The spectrum of eigenvalues is plotted in Fig. 4a for the Fourier-Laguerre problem, where the spherical Shannon number N_{PL} is also indicated, which confirms that the spherical Shannon number is indeed a good approximation of the number of significant eigenvalues. The spectrum of eigenvalues λ^1 and λ^2 is plotted in Fig. 4c and Fig. 4d respectively, where we have also indicated N^P and N_L . For the concentration problem in the Fourier-Laguerre domain, the measure of radial concentration (λ^1) is independently controlled by the radial band-limit P and angular concentration (λ^2) is controlled by the angular band-limit L . Consequently, concentration in the spatial region $R \subset \mathbb{B}^3$ is given by $\lambda = \lambda^1 \lambda^2$, due to which, the transition of the spectrum of eigenvalues λ from unity to zero is non-smooth⁶. However, the spectrum of each λ^1 and λ^2 does have a smooth transition, that is, the spectrum does not have step-like transitions. For the problem in the Fourier-Bessel domain, the transition is smooth due to the spectral coupling between radial and angular components, as discussed earlier.

For the Fourier-Bessel spectral domain, the first 12 most concentrated band-limited eigenfunctions $f^{(m)}(r, \theta)$ given in (64) for $m = 2$ are shown in the spatial domain in Fig. 5. The associated space-limited

⁶Non-smooth here refers to the observed step-like transitions in the spectrum of eigenvalues.

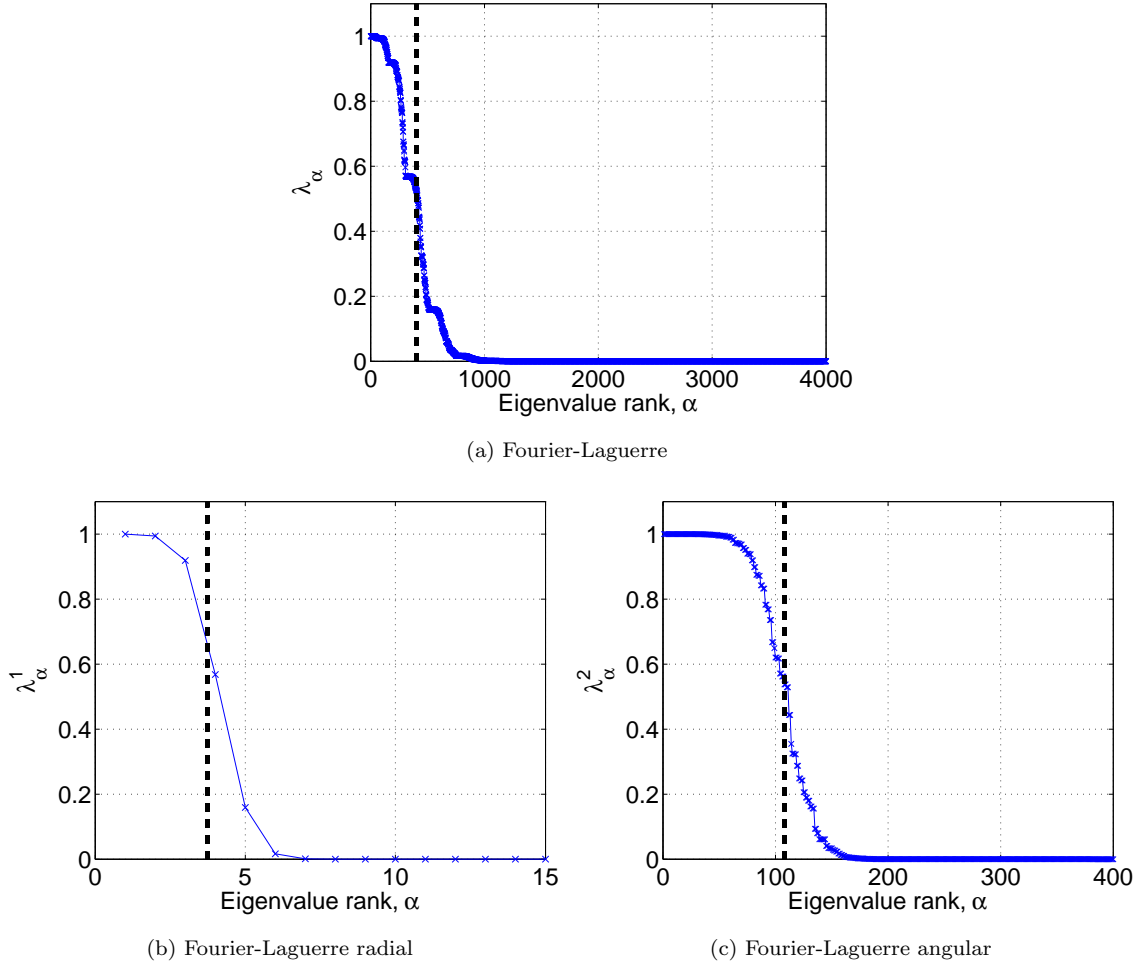


Figure 4: **Spectrum of eigenvalues for the Fourier-Laguerre domain eigenvalue problem** formulated in (48) to find spatially concentrated eigenfunctions band-limited in the Fourier-Laguerre domain in the spectral region $A_{(30,20)}$, plotted in (a). The spatial region of concentration is $R = \{15 \leq r \leq 25, \pi/8 \leq \theta \leq 3\pi/8, 0 \leq \phi < 2\pi\}$. Since the region is circularly symmetric and radially independent, the problem in the Fourier-Laguerre domain can be decomposed into two separate eigenvalue problems in radial and angular regions formulated in (77) and (78), for which the spectrum of eigenvalues is plotted in (b) and (c) respectively. Note that the transition of the eigenvalue spectrum from unity to zero in (b) is not smooth since the radial and angular components are interspersed. The sum of eigenvalues, given by the spherical Shannon number for each case is (a) $N_{PL} = 403.21$, (b) $N^P = 3.72$ and (c) $N_L = 108.24$, as indicated by the vertical dashed lines. The spherical Shannon numbers estimate the location of the transition in the eigenvalue spectrum accurately.

functions concentrated in the spectral domain are shown in Fig. 6, computed using (57) (note that these functions are not band-limited and so their spectral representation is non-zero outside of the plotted domain). For the Fourier-Laguerre domain, the first 12 most concentrated band-limited eigenfunctions $f^{(m)}(r, \theta)$ given in (68) for $m = 2$ are shown in the spatial domain in Fig. 7. The associated space-limited functions concentrated in the spectral domain are shown in Fig. 8, computed using (57) (again, note that these functions are not band-limited). For space-limited eigenfunctions, it can be noted that the leakage of concentration (en-

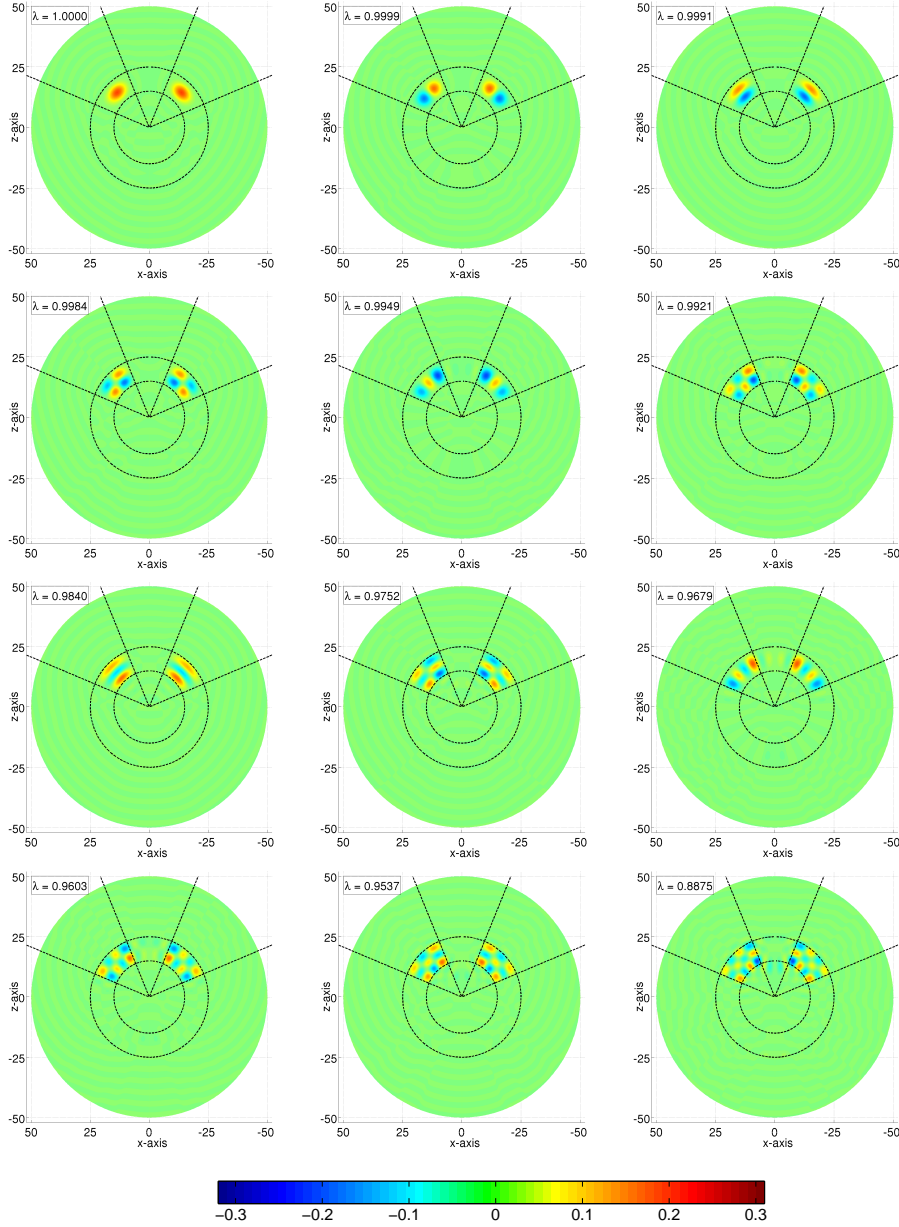


Figure 5: **Fourier-Bessel band-limited spatially concentrated eigenfunctions** $f^m(r, \theta)$ given in (64), obtained as solutions of the fixed-order eigenvalue problem in (63) for $m = 2$. Each eigenfunction $f^m(r, \theta)$ is independent of ϕ and is plotted for $r \leq 50$. The spatial region of concentration is $R = \{15 \leq r \leq 25, \pi/8 \leq \theta \leq 3\pi/8, 0 \leq \phi < 2\pi\}$ and is azimuthally symmetric and radially independent. The dependence of the eigenfunction in ϕ is $e^{im\phi}$, as given in (69). The eigenfunctions are band-limited in the Fourier-Bessel domain within the spectral region $\tilde{A}_{(1.4,20)}$. The eigenvalue λ associated with each eigenfunction is a measure of spatial concentration within the spatial region R .

ergy) outside the Fourier-Bessel spectral region of interest is diagonally spread due to the spectral coupling between the radial and angular components for the Fourier-Bessel functions. In contrast, the leakage outside the Fourier-Laguerre spectral region of interest has horizontally and/or vertically spread due to the separability of the radial and angular components of the Fourier-Laguerre functions.

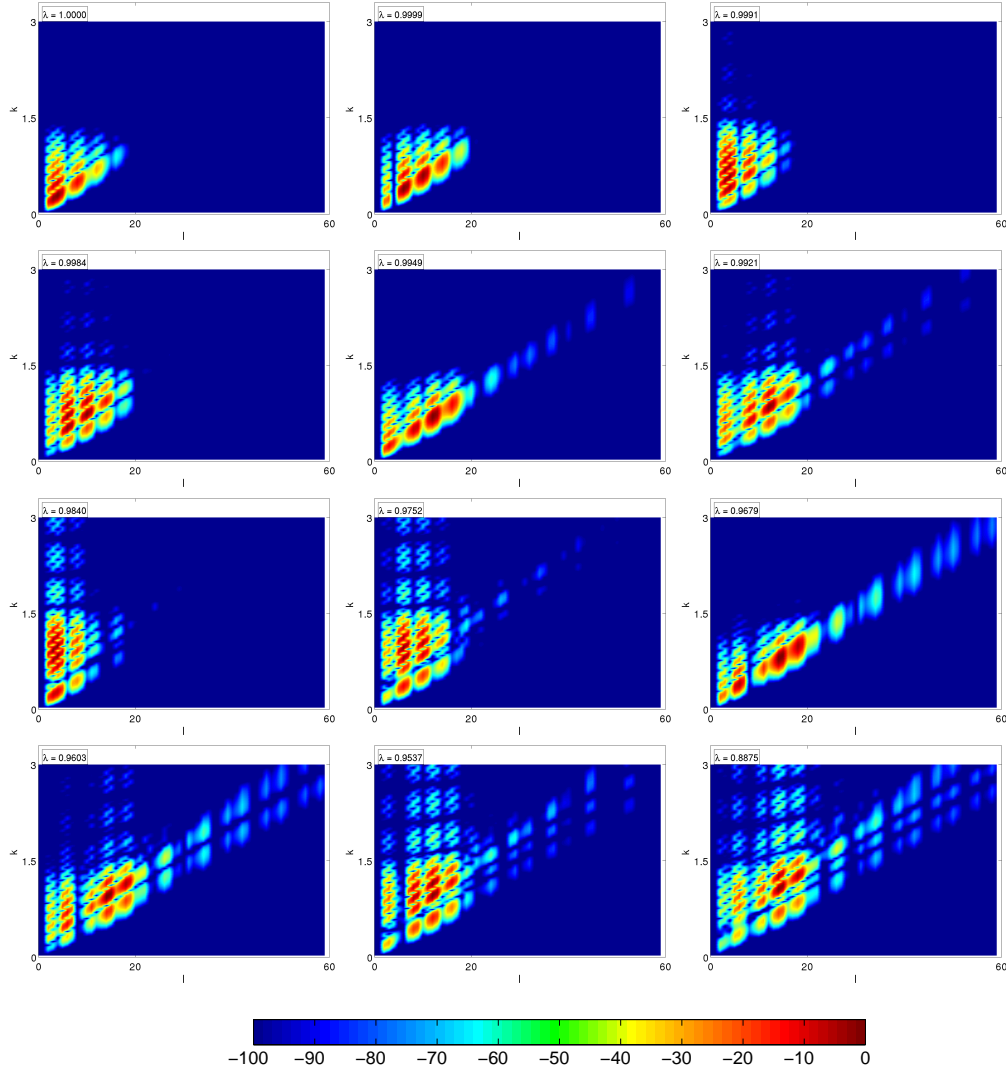


Figure 6: **Fourier-Bessel spectral domain response of space-limited spectrally concentrated eigenfunctions**, given by their magnitude square $|g_{\ell m}(k)|^2$. Each eigenfunction is limited in the azimuthally symmetric and radially independent spatial region $R = \{15 \leq r \leq 25, \pi/8 \leq \theta \leq 3\pi/8, 0 \leq \phi < 2\pi\}$ and spectrally concentrated in the Fourier-Bessel domain within the spectral region $\tilde{A}_{(1.4,20)}$. The eigenvalue λ associated with each eigenfunction is a measure of the spectral concentration within the Fourier-Bessel spectral domain $\tilde{A}_{(1.4,20)}$. The values of $|g_{\ell m}(k)|^2$ are plotted in decibels as $20 \log |g_{\ell m}(k)|$, normalized to zero at the individual maxima of each eigenfunction.

6. Representation of Signal in Slepian Basis

The eigenfunctions, band-limited in the Fourier-Bessel or Fourier-Laguerre spectral domain, form a complete orthonormal basis for signals band-limited in the respective domain. We call the band-limited eigenfunctions that arise as solutions of the eigenvalue problems (44) and (48) a *Slepian basis*. By completeness, any band-limited signal can be represented in the Slepian basis constructed with the same band-limit.

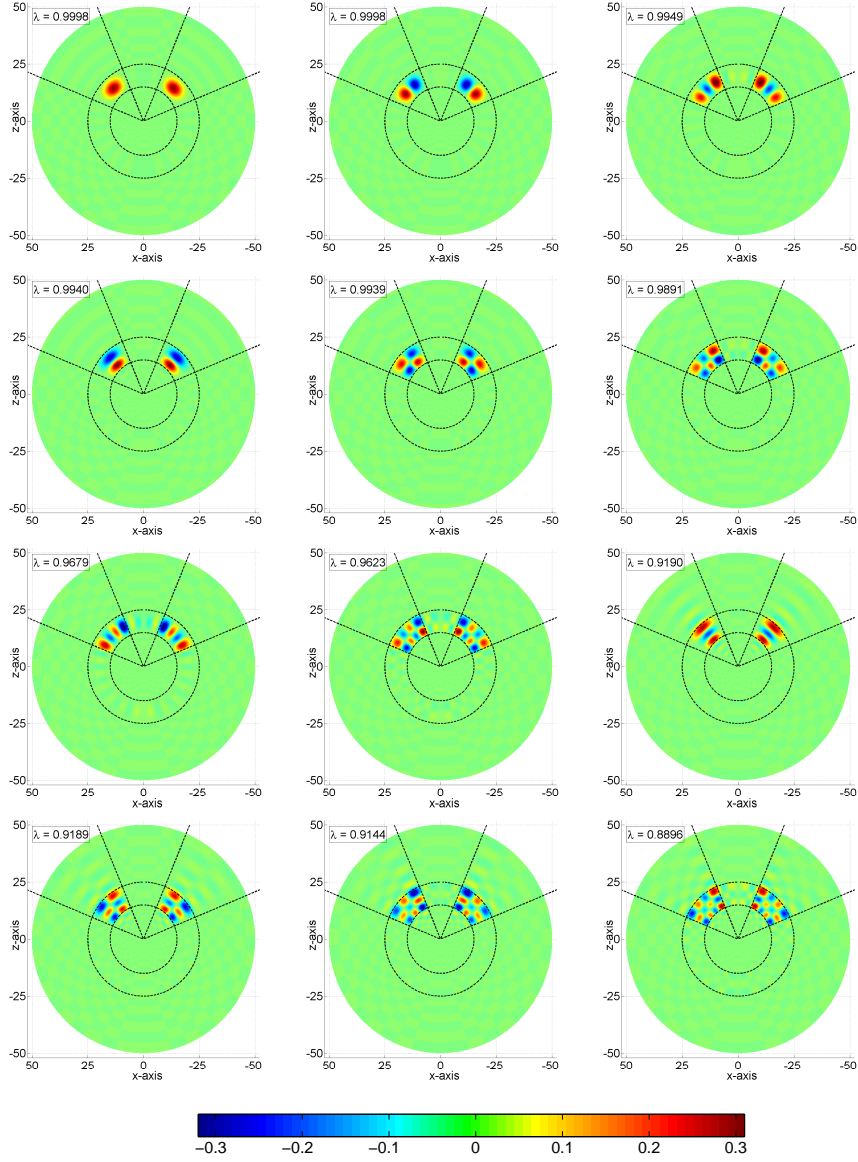


Figure 7: **Fourier-Laguerre band-limited spatially concentrated eigenfunctions** $f^m(r, \theta)$ given in (68), obtained as solutions of the fixed-order eigenvalue problem in (67) for $m = 2$. Each eigenfunction $f^m(r, \theta)$ is independent of ϕ and is plotted for $r \leq 50$. The spatial region of concentration is $R = \{15 \leq r \leq 25, \pi/8 \leq \theta \leq 3\pi/8, 0 \leq \phi < 2\pi\}$ and is azimuthally symmetric and radially independent. The dependence of the eigenfunction in ϕ is $e^{im\phi}$, as given in (69). The eigenfunctions are band-limited in the Fourier-Laguerre domain within the spectral region $A_{(30,20)}$. The eigenvalue λ associated with each eigenfunction is a measure of spatial concentration within the spatial region R .

A Fourier-Bessel band-limited signal $h \in \tilde{\mathcal{H}}_{KL} \subset L^2(\mathbb{B}^3)$ can thus be represented by

$$\begin{aligned}
 h(\mathbf{r}) &= \int_{k=0}^K dk \sum_{\ell=0}^{L-1} \sum_{m=-\ell}^{\ell} h_{\ell m}(k) X_{\ell m}(k, \mathbf{r}) \\
 &= \sum_{\alpha=1}^{J_C} h_{\alpha} f^{\alpha}(\mathbf{r}), \quad f^{\alpha}, h \in \tilde{\mathcal{H}}_{KL},
 \end{aligned} \tag{86}$$

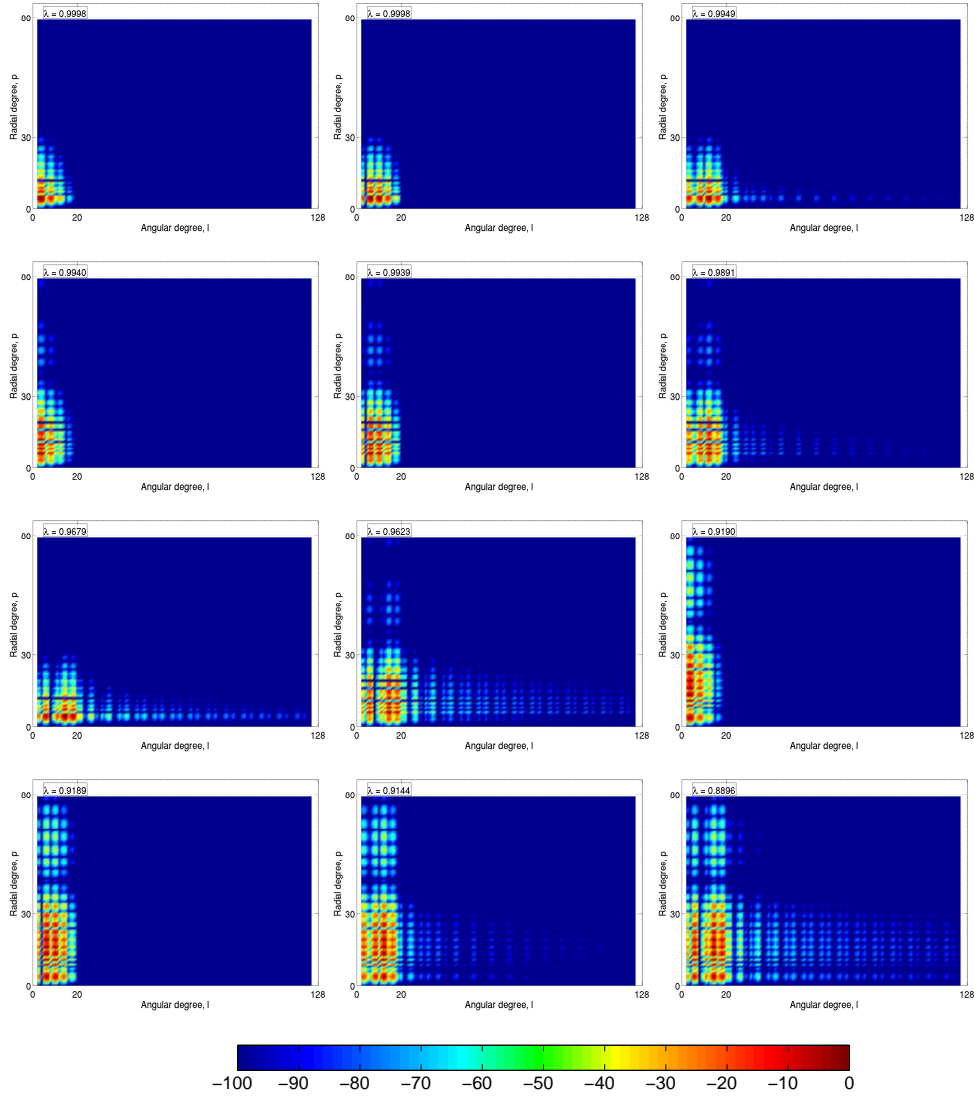


Figure 8: **Fourier-Laguerre spectral domain response of space-limited spectrally concentrated eigenfunctions**, given by their magnitude square $|g_{\ell m p}|^2$. Each eigenfunction is limited in the azimuthally symmetric and radially independent spatial region $R = \{15 \leq r \leq 25, \pi/8 \leq \theta \leq 3\pi/8, 0 \leq \phi < 2\pi\}$ and spectrally concentrated in the Fourier-Laguerre domain within the spectral region $A_{(30,20)}$. The eigenvalue λ associated with each eigenfunction is a measure of the spectral concentration within the Fourier-Laguerre spectral domain $A_{(30,20)}$. The values of $|g_{\ell m p}|^2$ are plotted in decibels as $20 \log |g_{\ell m p}|$, normalized to zero at the individual maxima of each eigenfunction.

and a Fourier-Laguerre band-limited signal $h \in \mathcal{H}_{PL} \subset L^2(\mathbb{B}^3)$ can be represented by

$$\begin{aligned}
 h(\mathbf{r}) &= \sum_{p=0}^{P-1} \sum_{\ell=0}^{L-1} \sum_{m=-\ell}^{\ell} h_{\ell m p} Z_{\ell m p}(\mathbf{r}) \\
 &= \sum_{\alpha=1}^{J_C} h_{\alpha} f^{\alpha}(\mathbf{r}), \quad f^{\alpha}, h \in \mathcal{H}_{PL},
 \end{aligned} \tag{87}$$

where h_α denotes the Slepian coefficient given by

$$h_\alpha = \int_{\mathbb{B}^3} d^3\mu(r) h(\mathbf{r}) (f^\alpha(\mathbf{r}))^* \quad (88)$$

(we use a single subscript to denote Slepian coefficients, similar to the notation used to denote spherical Laguerre coefficients; however, the case intended should be obvious from the context). In (86) and (87), $J_C = ML^2$ and $J_C = PL^2$, respectively, denotes the number of band-limited eigenfunctions that serve as complete orthonormal basis for the subspace $\tilde{\mathcal{H}}_{KL}$ or \mathcal{H}_{PL} . Here $M = \lceil K/\Delta k \rceil$ with Δk denoting the step size used for the discretization of the continuous spectrum along k . Note that the signal h and the eigenfunctions f^α belong to the same subspace. We note that the Slepian coefficient in (88) can also be obtained through the spectral domain representation of both signal and Slepian basis function, that is, by

$$\begin{aligned} h_\alpha &= \sum_{\ell=0}^{L-1} \sum_{m=-\ell}^{\ell} \int_{k=0}^K dk h_{\ell m}(k) (f_{\ell m}^\alpha(k))^*, \quad f^\alpha, h \in \tilde{\mathcal{H}}_{KL} \\ h_\alpha &= \sum_{p=0}^{P-1} \sum_{\ell=0}^{L-1} \sum_{m=-\ell}^{\ell} h_{\ell mp} (f_{\ell mp}^\alpha)^*, \quad f^\alpha, h \in \mathcal{H}_{PL}. \end{aligned} \quad (89)$$

When a band-limited signal is spatially concentrated in some spatial region R , it can be approximated by the number of significant eigenfunctions that are well concentrated in the spatial region R . Since the eigenvalue associated with each eigenfunction is a measure of concentration in the spatial region R and the eigenfunctions f^α are indexed such that $\lambda_\alpha \geq \lambda_{\alpha+1}$, a band-limited signal concentrated in the spatial region R can be approximated accurately by truncating the summation over the Slepian basis functions in (86) and (87) at the truncation level J_T such that $\lambda_{J_T+1} \approx 0$, that is,

$$h(\mathbf{r}) \approx \sum_{\alpha=1}^{J_T} h_\alpha f^\alpha(\mathbf{r}), \quad (90)$$

where the same region R is used to construct the eigenfunctions. It also follows that the Slepian coefficients associated with the remaining eigenfunctions (which are concentrated in the region $\mathbb{B}^3 \setminus R$) are close to zero. Consequently, a concentrated signal is *sparse*⁷ when represented in the Slepian basis, where the degree of sparsity is quantified by the number of significant eigenfunctions with eigenvalues close to unity. The representation of a concentrated signal in the Slepian basis, truncated J_T , can thus give considerable savings in terms of the number of coefficients required to represent the signal accurately.

The accuracy of the approximate representation of the signal within the spatial region R can be quantified by the ratio of the energy of the approximate representation to the energy of the exact representation within

⁷Formally the signal is *compressible* since the Slepian coefficients associated with the remaining eigenfunctions are small and not identically zero.

the region R . We define such an accuracy measure by

$$Q(J_T) = \frac{\int_R d^3\mu(\mathbf{r}) \left| \sum_{\alpha=1}^{J_T} h_\alpha f^\alpha(\mathbf{r}) \right|^2}{\int_R d^3\mu(\mathbf{r}) \left| \sum_{\alpha=1}^{J_C} h_\alpha f^\alpha(\mathbf{r}) \right|^2} = \frac{\sum_{\alpha=1}^{J_T} \lambda_\alpha |h_\alpha|^2}{\sum_{\alpha=1}^{J_C} \lambda_\alpha |h_\alpha|^2}, \quad (91)$$

where we have used the orthogonality relationships given in (51) and (54) in obtaining the second equality. The closer the value of $Q(J_T)$ to unity, the greater the accuracy of the approximate representation of signal within the spatial region R . Since the truncation level is chosen such that $\lambda_{J_T+1} \approx 0$, the accuracy of the approximation within the spatial region R is high.

Since the spherical Shannon numbers approximately represent the number of significant band-limited eigenfunctions that are well concentrated in the spatial region R , the summation over the Slepian basis functions in (86) and (87) can be truncated at the spherical Shannon numbers \tilde{N}_{KL} and N_{PL} , respectively, that is, $J_T = \tilde{N}_{KL}$ for $f^\alpha, h \in \tilde{\mathcal{H}}_{KL}$ and $J_T = N_{PL}$ for $f^\alpha, h \in \mathcal{H}_{PL}$. The truncation at the spherical Shannon number is based on an assumption that the spectrum of eigenvalues has narrow-width transition from unity to zero. For the cases when this assumption is not fairly supported, the spherical Shannon number can be used as a measure to determine a truncation level J_T greater than the spherical Shannon number such that all of the eigenfunctions are included in the truncated representation given in (90). In such cases, the difference between the truncation level J_T and the spherical Shannon number depends on the spatial region of interest and the desired accuracy required for the representation of the signal in the Slepian basis. In the next section, we provide an illustration to demonstrate that truncation at the spherical Shannon number gives a sufficiently accurate representation of the signal within the spatial region R . Finally, we note that truncation at the spherical Shannon number has also been adopted for the representation of signals in the Slepian basis defined for multi-dimensional Euclidean domains and various geometries (e.g., [36, 39, 51]).

6.1. Illustration

We present an example to illustrate the fact that the representation of a spatially concentrated band-limited signal in the Slepian basis is sparse. We consider a test signal obtained from a simulation of the dark matter distribution of the Universe, observed over a partial field-of-view. Specifically, the test signal is extracted from the full-sky Horizon Simulation [45], an N -body simulation that covers a 1Gpc periodic box of 70 billion dark matter particles generated from the cosmological concordance model derived from 3-year Wilkinson Microwave Anisotropy Probe (WMAP) observations [44]. We limit the data in the spatial domain with an Sloan Digital Sky Survey (SDSS) DR7⁸ quasar binary mask on the sphere, denoted by $R_s \subset \mathbb{S}^2$, and in the interval $15 \leq r \leq 25$ along the radial line (note that the units of radius for the data

⁸<http://www.sdss.org/dr7/>

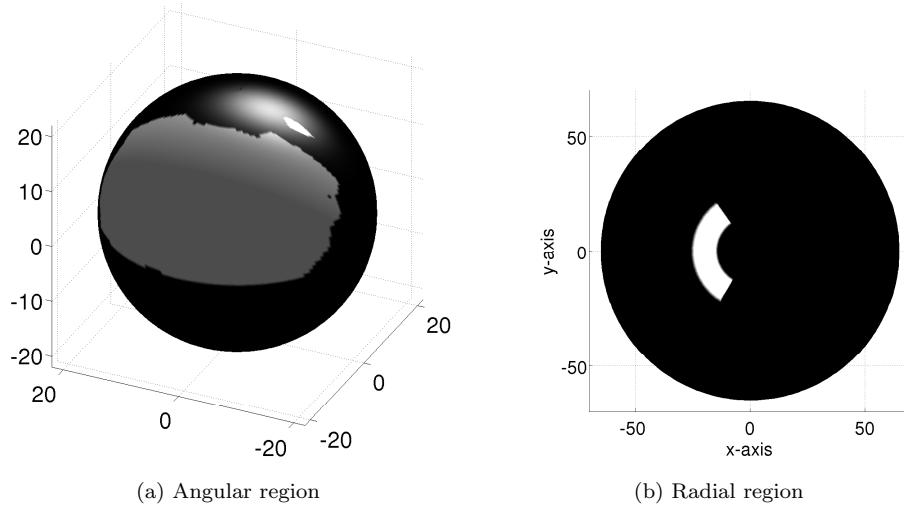


Figure 9: **Non-trivial spatial region** constructed from (a) the SDSS DR7 quasar mask on the sphere (shown on the sphere of radius $r = 20$) and (b) a radial profile limited to the interval $15 \leq r \leq 25$ (shown in the x - y plane).

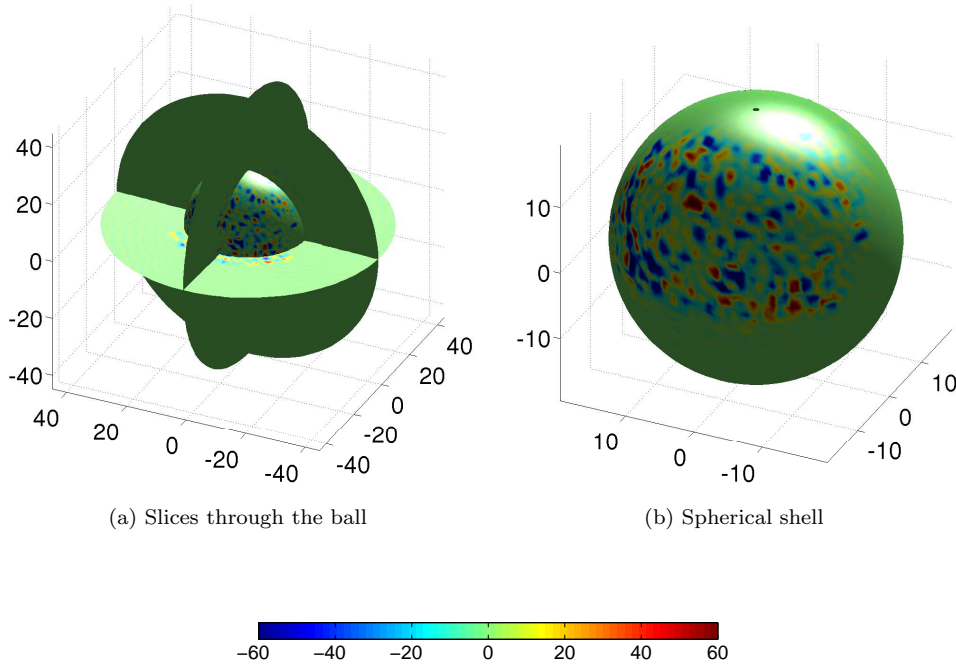


Figure 10: **Simulated dark matter density test signal on the ball**, band-limited and spatially concentrated in the region shown in Fig. 9. The test signal $h \in \mathcal{H}_{PL} \subset L^2(\mathbb{B}^3)$ is band-limited in the Fourier-Laguerre domain at angular degree $L = 72$ and radial degree $P = 144$, and spatially concentrated in the angular region defined by the SDSS DR7 quasar mask and radially in the interval $15 \leq r \leq 25$. The test signal is plotted on (a) slices through the ball and (b) on a spherical shell at $r = 20$.

under consideration are Mpc). The resulting mask is shown in Fig. 9. The masked signal is band-limited at $L = 72$ and $P = 144$ to obtain the spatially concentrated band-limited test signal $h \in \mathcal{H}_{PL}$ shown in Fig. 10.

The region considered is not symmetric but is radially independent, hence we compute the band-limited eigenfunctions separately on the radial line over the interval $15 \leq r \leq 25$ with band-limit $P = 144$ and on the sphere over the region R_s with band-limit $L = 72$. In total, $PL^2 = 746\,496$ eigenfunctions $f^\alpha \in \mathcal{H}_{PL}$ are computed. The spectrum of eigenvalues is plotted in Fig. 11 for the first 16 000 eigenvalues only, where the spherical Shannon number $\lfloor N_{PL} \rfloor = 8\,696$ is also indicated, which is computed using (85).

Since the eigenfunctions f^α serve as a complete basis for the subspace \mathcal{H}_{PL} , the signal h can be alternatively represented in the Slepian basis as given in (87), where we compute the Slepian coefficients h_α using (89). Recall that \mathcal{H}_{PL} is a PL^2 dimensional subspace, thus there are PL^2 spectral coefficients $h_{\ell mp}$ or Slepian coefficients h_α . The decay of the Fourier-Laguerre coefficients $h_{\ell mp}$ and the Slepian coefficients h_α is compared in Fig. 12, where both are first sorted and then plotted. As expected, the Slepian coefficients decay much more rapidly than the Fourier-Laguerre coefficients. The spatially concentrated signal indeed has a very sparse representation in the Slepian basis; it can be represented accurately within the spatial region of interest with only $\lfloor N_{PL} \rfloor = 8\,696$ Slepian coefficients, compared to the full dimensionality of the subspace of $PL^2 = 746\,496$. The energy ratio captured by the approximate representation, defined by the accuracy measure of (91), is $Q(N_{PL}) = 99.73\%$, again indicating that the approximation is sufficiently accurate within the spatial region of interest.

Our code to solve the eigenvalue problems that result from the Slepian spatial-spectral concentration problem on the ball, and used to perform the illustrations presented here, is publicly available.⁹

7. Conclusions

We have formulated and solved the Slepian spatial-spectral concentration problem on the ball. We consider two domains for the spectral characterization of the signal defined on the ball, namely the Fourier-Bessel domain and the Fourier-Laguerre domain. The Fourier-Laguerre domain is considered in addition to the standard Fourier-Bessel domain since the former has a number of practical advantages. The orthogonal families of band-limited spatially concentrated functions and of space-limited spectrally concentrated functions can be computed as solutions of eigenvalue problems. The spatially and spectrally concentrated eigenfunctions that arise as solutions of these eigenvalue problems coincide with each other inside both the spatial and spectral regions of interest. The eigenvalue associated with each eigenfunction is a measure of both the spatial concentration of the band-limited function and of the spectral concentration of the space-limited function. The number of well-concentrated (significant) eigenfunctions depends on the spherical

⁹<http://astro-informatics.github.io/b3slep>

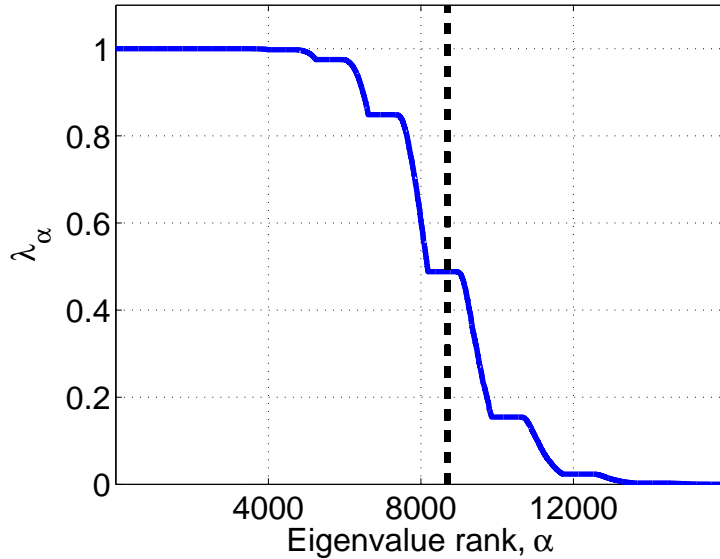


Figure 11: **Spectrum of eigenvalues λ_α for the non-trivial region** associated with the band-limited spatially concentrated eigenfunctions. The angular band-limit $L = 72$ and radial band-limit $P = 144$ are assumed, while the spatial region shown in Fig. 9 is considered, i.e. defined by the SDSS DR7 quasar mask on the sphere and the radial interval $15 \leq r \leq 25$. The horizontal axis is truncated to show only the first 16 000 eigenvalues (out of the total of 746 496 eigenvalues). The spherical Shannon number $[N_{PL}] = 8\,696$ is also indicated by the vertical dashed line. Note, again, that the transition of the eigenvalue spectrum from unity to zero is not smooth since the radial and angular components are interspersed. The spherical Shannon number again estimates the location of the transition in the eigenvalue spectrum accurately.

Shannon number, which also serves as the dimension of the space of functions that can be concentrated in both the spatial and spectral domains at the same time. When the spatial region of interest is rotationally symmetric and/or radially independent, the eigenvalue problem decomposes into subproblems, which reduces the computational burden. This reduction in the computational complexity is significant for the concentration problem in the Fourier-Laguerre spectral domain and radially independent spatial regions, where the independence between the radial and angular components of the basis functions completely decouples the problem to find band-limited eigenfunctions such that they can be independently concentrated along radial component and angular component. The family of concentrated eigenfunctions can be used to form an orthonormal basis, or Slepian basis, which provides a sparse representation of concentrated functions.

Just as the Slepian basis in the one-dimensional Euclidean domain and other geometries have proven to be extremely valuable, we hope the Slepian eigenfunctions on the ball developed in this work will prove useful in a variety of applications in various fields of science and engineering (e.g., geophysics, cosmology and planetary science), where signals are inherently defined on the ball. Some applications where the proposed orthogonal family of eigenfunctions (Slepian basis) are likely to be of use are the estimation of signals, their power spectrum, and other statistics, when noisy observations on the ball can only be made over partial fields-of-views. For example, surveys of the distribution of galaxies in our Universe are observed only over

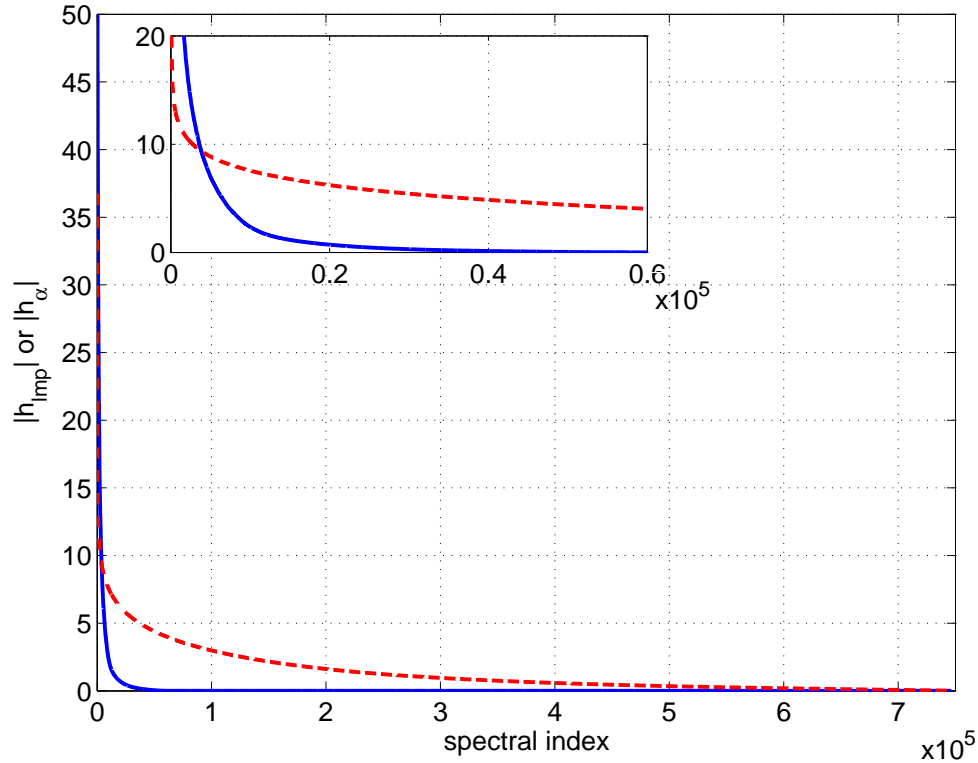


Figure 12: **Spectral decay of the Fourier-Laguerre (red dashed line) and Slepian coefficients (blue solid line)** of the band-limited spatially concentrated test signal shown in Fig. 10. The absolute values of both the Fourier-Laguerre $h_{\ell mp}$ and Slepian h_{α} coefficients are first sorted in descending order and then plotted. Since the band-limited signal h is spatially concentrated, it has a sparse representation in the Slepian basis.

partial fields-of-view [2] on the ball, while their statistical properties can be used to infer the physics of our Universe, such as the nature of dark energy and dark matter.

Acknowledgements

We thank Hiranya Peiris and Boris Leistedt for useful discussions, for providing the processed Horizon simulation data-set, and for their hospitality during the visit of Z. Khalid to UCL.

- [1] Abramo, L. R., Reimberg, P. H., Xavier, H. S., Aug 2010. CMB in a box: Causal structure and the Fourier-Bessel expansion. *Phys. Rev. D* 82, 043510.
- [2] Ahn, C. P., Alexandroff, R., Allende Prieto, C., Anderson, S. F., Anderton, T., Andrews, B. H., Aubourg, É., Bailey, S., Balbinot, E., Barnes, R., et al., Dec. 2012. The Ninth Data Release of the Sloan Digital Sky Survey: First Spectroscopic Data from the SDSS-III Baryon Oscillation Spectroscopic Survey. *Astrophys. J. Supp.* 203, 21.
- [3] Albertella, A., Sansò, F., Sneeuw, N., Jun. 1999. Band-limited functions on a bounded spherical domain: the Slepian problem on the sphere. *J. Geodesy* 73 (9), 436–447.
- [4] Amore, P., 2005. Asymptotic and exact series representations for the incomplete Gamma function. *Europhys. Lett.* 71 (1), 1–7.

- [5] Boyd, J. P., 2003. Approximation of an analytic function on a finite real interval by a bandlimited function and conjectures on properties of prolate spheroidal functions. *Appl. Comp. Harm. Anal.* 15 (2), 168–176.
- [6] Castro, P. G., Heavens, A. F., Kitching, T. D., Jul. 2005. Weak lensing analysis in three dimensions. *Phys. Rev. D.* 72 (2), 023516.
- [7] Chen, Q., Gottlieb, D., Hesthaven, J., 2005. Spectral methods based on prolate spheroidal wave functions for hyperbolic PDEs. *SIAM J. on Numer. Anal.* 43 (5), 1912–1933.
- [8] Cohen, L., Jul. 1989. Time-frequency distributions-a review. *Proc. IEEE* 77 (7), 941–981.
- [9] Colton, D., Kress, R., 1998. *Inverse Acoustic and Electromagnetic Scattering Theory*, 2nd Edition. Springer-Verlag, Berlin.
- [10] Dahlen, F. A., Simons, F. J., 2008. Spectral estimation on a sphere in geophysics and cosmology. *Geophys. J. Int.* 174, 774–807.
- [11] Daubechies, I., 1988. Time-frequency localization operators: a geometric phase space approach. *IEEE Trans. Inf. Theory* 34 (4), 605–612.
- [12] Daubechies, I., 1990. The wavelet transform, time-frequency localization and signal analysis. *IEEE Trans. Inf. Theory* 36 (5), 961–1005.
- [13] de Villiers, G. D., Marchaud, F. B. T., Pike, E. R., 2001. Generalized Gaussian quadrature applied to an inverse problem in antenna theory. *Inverse Probl.* 17 (4), 1163–1179.
- [14] dunkl, C. F., 2003. A Laguerre polynomial orthogonality and the hydrogen atom. *Anal. and Appl.* 01 (02), 177–188.
- [15] Jackson, J. I., Meyer, C. H., Nishimura, D. G., Macovski, A., 1991. Selection of a convolution function for Fourier inversion using gridding [computerised tomography application]. *IEEE Trans. Med. Imag.* 10 (3), 473–478.
- [16] Kennedy, R. A., Sadeghi, P., Mar. 2013. *Hilbert Space Methods in Signal Processing*. Cambridge University Press, Cambridge, UK.
- [17] Landau, H. J., 1975. On Szegő's eigenvalue distribution theorem and non-Hermitian kernels. *J. Analyse Math.* 28 (1), 335–357.
- [18] Landau, H. J., O.Pollak, H., Jan. 1961. Prolate spheroidal wave functions, Fourier analysis and uncertainty-II. *Bell System Tech J.* 40, 65–84.
- [19] Landau, H. J., O.Pollak, H., 1962. Prolate spheroidal wave functions, Fourier analysis and uncertainty-III: The dimension of the space of essentially time- and band-limited signals. *Bell System Tech J.* 41, 1295–1336.
- [20] Landau, H. J., Widom, H., 1980. Eigenvalue distribution of time and frequency limiting. *Journal of Mathematical Analysis and Applications* 77 (2), 469–481.
- [21] Lanusse, F., Rassat, A., Starck, J.-L., Apr. 2012. Spherical 3D isotropic wavelets. *Astron. & Astrophys.* 540, A92.
- [22] Leistedt, B., McEwen, J. D., 2012. Exact wavelets on the ball. *IEEE Trans. Sig. Proc.* 60 (12), 6257–6269.
- [23] Leistedt, B., Rassat, A., Rfrgier, A., Starck, J.-L., Apr. 2012. 3DEX: a code for fast spherical Fourier-Bessel decomposition of 3D surveys. *Astron. & Astrophys.* 540, A60.
- [24] Lemoine, D., 1994. The discrete bessel transform algorithm. *J Chem. Phys* 101 (5), 3936–3944.
- [25] Mathews, J., Breakall, J., Karawas, G., 1985. The discrete prolate spheroidal filter as a digital signal processing tool. *IEEE Trans. Acoust., Speech, Signal Process.* 33 (6), 1471–1478.
- [26] McEwen, J. D., Wiaux, Y., Dec. 2011. A novel sampling theorem on the sphere. *IEEE Trans. Signal Process.* 59 (12), 5876–5887.
- [27] Meaney, C., 1984. Localization of spherical harmonic expansions. *Monatsh. Math.* 98 (1), 65–74.
- [28] Moore, I. C., Cada, M., 2004. Prolate spheroidal wave functions, an introduction to the Slepian series and its properties. *Appl. Comp. Harm. Anal.* 16 (3), 208–230.
- [29] Mortlock, D. J., Challinor, A. D., Hobson, M. P., Feb. 2002. Analysis of cosmic microwave background data on an incomplete sky. *Mon. Not. Roy. Astron. Soc.* 330, 405–420.

- [30] N. Fernandez, 2003. Polynomial bases on the sphere. In: *Advanced Problems in Constructive Approximation*. Vol. 142 of ISNM Inter. Ser. Numer. Math. Birkhuser Basel, pp. 39–52.
- [31] Percival, D., Walden, A., 1993. *Spectral analysis for physical applications: multitaper and conventional univariate techniques*. Cambridge University Press, Cambridge, New York.
- [32] Pollard, H., Apr. 1947. Representation of an analytic function by a Laguerre series. *Annals of Mathematics* 48 (2), 358–365.
- [33] Sakurai, J. J., 1994. *Modern Quantum Mechanics*, 2nd Edition. Addison Wesley Publishing Company, Inc., Reading, MA.
- [34] Shkolnisky, Y., 2007. Prolate spheroidal wave functions on a disc - integration and approximation of two-dimensional bandlimited functions. *Appl. Comp. Harm. Anal.* 22 (2), 235 – 256.
- [35] Shkolnisky, Y., Tygert, M., Rokhlin, V., 2006. Approximation of bandlimited functions. *Appl. Comp. Harm. Anal.* 21 (3), 413 – 420.
- [36] Simons, F. J., Dahlen, F. A., Wieczorek, M. A., 2006. Spatiospectral concentration on a sphere. *SIAM Rev.* 48 (3), 504–536.
- [37] Simons, F. J., Loris, I., Brevdo, E., Daubechies, I. C., 2011. Wavelets and wavelet-like transforms on the sphere and their application to geophysical data inversion. In: *Wavelets and Sparsity XIV*. Vol. 81380. SPIE, p. 81380X.
- [38] Simons, F. J., Loris, I., Nolet, G., Daubechies, I. C., Voronin, S., Vetter, P. A., Charlty, J., Vonesch, C., 2011. Solving or resolving global tomographic models with spherical wavelets, and the scale and sparsity of seismic heterogeneity. *Geophys. J. Int.* 187, 969–988.
- [39] Simons, F. J., Wang, D. V., 2011. Spatiospectral concentration in the cartesian plane. *Intern. J. Geomath.* 2 (1), 1–36.
- [40] Slepian, D., 1964. Prolate spheroidal wave functions, Fourier analysis and uncertainty-IV: Extensions to many dimensions; generalized prolate spheroidal functions. *Bell Syst. Tech. J* 43, 3009–3057.
- [41] Slepian, D., 1983. Some comments on Fourier analysis, uncertainty and modeling. *SIAM Review* 25 (3), 379–393.
- [42] Slepian, D., Pollak, H. O., Jan. 1961. Prolate spheroidal wave functions, Fourier analysis and uncertainty-I. *Bell Systems Technical Journal* 40, 43–63.
- [43] Slepian, D., Sonnenblick, E., 1965. Eigenvalues associated with prolate spheroidal wave functions of zero order. *Bell System Technical Journal* 44 (8), 1745–1759.
- [44] Spergel, D. N., Bean, R., Doré, O., Nolta, M. R., Bennett, C. L., Dunkley, J., Hinshaw, G., Jarosik, N., Komatsu, E., Page, L., Peiris, H. V., Verde, L., Halpern, M., Hill, R. S., Kogut, A., Limon, M., Meyer, S. S., Odegard, N., Tucker, G. S., Weiland, J. L., Wollack, E., Wright, E. L., 2007. Three-year Wilkinson Microwave Anisotropy Probe (WMAP) observations: Implications for cosmology. *The Astrophysical Journal Supplement Series* 170 (2), 377–408.
- [45] Teyssier, R., Pires, S., Prunet, S., Aubert, D., Pichon, C., Amara, A., Benabed, K., Colombi, S., Refregier, A., Starck, J.-L., Apr. 2009. Full-sky weak-lensing simulation with 70 billion particles. *Astron. & Astrophys.* 497 (2), 335–341.
- [46] Thomson, D. J., 1982. Spectrum estimation and harmonic analysis. *Proc. IEEE* 70 (9), 1055–1096.
- [47] Thomson, D. J., 1990. Quadratic-inverse spectrum estimates: Applications to Palaeoclimatology. *Philos. Trans. R. Soc. of Lond. Ser. A* 332 (1627), 539–597.
- [48] Thomson, D. J., Robbins, M. F., MacLennan, C. G., Lanzerotti, L. J., 1976. Spectral and windowing techniques in power spectral analyses of geomagnetic data. *Physics of the Earth and Planetary Interiors* 12 (23), 217 – 231.
- [49] Watson, G., 1995. *A treatise on the theory of Bessel functions*, 2nd Edition. Cambridge University Press.
- [50] Weniger, E. J., 2008. On the analyticity of Laguerre series. *J. Phys. A: Math.Theor.* 41 (42), 425207.
- [51] Wieczorek, M. A., Simons, F. J., May 2005. Localized spectral analysis on the sphere. *Geophys. J. Int.* 162 (3), 655–675.
- [52] Wieczorek, M. A., Simons, F. J., 2007. Minimum variance multitaper spectral estimation on the sphere. *J. Fourier Anal. Appl.* 13 (6), 665–692.
- [53] Xu, W., Chanzas, C., 1983. On the extrapolation of band-limited functions with energy constraints. *IEEE Trans. Acoust., Speech, Signal Process.* 31 (5), 1222–1234.